TR 64-133

TECHNICAL REPORT NO. 64-133

GALVANOMETERS, PROJECT VT/072

DISTRIBUTION OF THIS
DOCUMENT IS UNLIMITED.

GEOTECH

THE GEOTECHNICAL CORPORATION

3401 SHILOH ROAD GARLAND, TEXAS

TECHNICAL REPORT NO. 64-133

GALVANOMETERS, PROJECT VT/072

by

B. M. Kirkpatrick

and

John Masse'

THE GEOTECHNICAL CORPORATION
3401 Shiloh Road
Garland, Texas

17 December 1964

IDENTIFICATION

AFTAC Project No: VT/072
Project Title: Improved Seismographs
ARPA Order No: 104-60
ARPA Code No: 8100
Contractor: The Geotechnical Corporation, Garland, Texas
Date of Contract: 1 November 1962
Amount of Contract: $852,675.00
Contract Number: AF 33(657)-9967
Contract Expiration Date: 31 October 1964
Project Engineer: J. R. Womack, BR8-8102

CONTENTS

CONTENTS, Continued

ILLUSTRATIONS

ILLUSTRATIONS, Continued

GALVANOMETERS, PROJECT VT/072

by

B. M. Kirkpatrick
and
John Masse'

ABSTRACT

Air damping in long-period galvanometers has been reduced by a moving-magnet fixed-coil design, wherein the moving magnet is operated in an evacuated glass housing. The susceptibility of this arrangement to influence by local magnetic fields was minimized by use of a rotor assembly employing a multiplicity of magnetic poles evenly distributed around two ring magnets. Magnetic polarization of materials in the immediate vicinity of the ring magnets was controlled by continuous high-frequency degaussing. Testing of the moving-magnet galvanometer was not fully completed. Preliminary tests indicate that the influence of local magnetic fields has not been entirely eliminated. There appears to be no advantage to the moving-magnet galvanometer over the usual moving-coil design at free periods up to 100 sec. However, the moving-magnet galvanometer shows promise at periods in excess of 100 sec where the air damping in normal moving-coil designs becomes excessive. For dependable use, the galvanometer needs to be properly oriented in the local magnetic field.

A computing or dynamometer-type galvanometer has been constructed and tested for use in seismic data analysis where a power-level indication is of interest and in signal multiplication and correlation. The galvanometer frequency response is independent of the circuit resistance and is controlled by fluid damping. When adjusted to give 0.7 of critical the apparent resonant frequency is 8.2 Hz.

An analysis was made of various optical factors governing the sensitivity of galvanometers with emphasis being placed on improving the sensitivity. Linear lateral and rotational magnifications were examined, using mirrors in both single and multiple reflections. Single- and double-pass lens systems using plane and spherical mirrors were studied.

BLANK PAGE

GALVANOMETERS. PROJECT VT/072

1. INTRODUCTION

1.1 GENERAL

This report describes the results of work performed under three subtasks as follows:

Reduce air damping;
Power-level galvanometer;
High-resolution galvanometer.

1.2 AUTHORIZATION

The work described here was performed in fulfillment of the requirement of Task 1b of VELA-UNIFORM Project VT/072, Contract AF 33(657)-9967 The project is under the technical direction of the Air Force Technical Applications Center (AFTAC) and under the overall direction of the Advanced Research Projects Agency (ARPA).

1.3 BACKGROUND

1.3.1 Reduce Air Damping

Air damping limits the sensitivity that can be realized in long-period galvanometers. As the period is increased, the air damping is increased until it eventually can constitute the larger part of the total damping. As a limit, the open-circuited galvanometer will be critically damped by air alone when the period is sufficiently long. In the case of the Harris Galvanometer, Model 8530-1, this limit is calculated to occur at a free period of approximately 300 sec. While this period is longer than any currently required, reduction of air damping at periods in the region of 100 sec would result in useful sensitivity improvements.

1.3.2 Power-Level Galvanometer

Power responsive or computing galvanometers may be useful in the analysis of seismic signals. Added information such as the determination of phase arrivals, power-level indication, and signal multiplication and correlation, could be provided by such a unit.

A pencil galvanometer, modified as a dynamometer, was originally contemplated. This unit would have been used in an automatic processing and recording camera (Develocorder). A dynamometer of this size proved to be impractical. A successful unit was subsequently designed which is a direct physical replacement for Model 16259 galvanometers in Model 16956 photocell amplifiers.

1.3.3 High-Resolution Galvanometer

The usefulness of the Harris galvanometer is somewhat limited by its relatively low sensitivity in direct recording applications. High mechanical and temperature stability was obtained in this design at some sacrifice in its sensitivity. It is desirable to maintain galvanometer stability by improving sensitivity by optical or other means. Extension of the effective optical lever by multiple reflections or by curved mirrors is a possible solution.

2. REDUCE AIR DAMPING

2.1 GENERAL

The air damping normally associated with long-period galvanometers has been reduced by an unusual moving-magnet fixed-coil design, wherein the moving magnet is enclosed in an evacuated glass housing. Fixed coils are arranged on the outside of the housing to control the magnet position and electromagnetic damping.

The sensitivity of long-period galvanometers is limited, to a degree, by air damping. The lower the air or open-circuit damping, the higher the sensitivity can be made. For any given design, sensitivity reaches a maximum when the air damping is zero

Galvanometer damping is made up of two parts: the open-circuit damping and the electromagnetic damping. The open-circuit damping is related to the mechanical design features of the galvanometer, such as the coil frontal area and the dimensions of the air space through which the coil moves. The open-circuit damping increases as the period increases. The electromagnetic damping is related to the magnetic flux density of the air gap in which the coil operates. The electromagnetic damping increases as the period increases and varies directly as the square of the flux density.

A reduction in air damping requires that an increase in the magnet flux level be made if the overall damping and circuit resistance are to be held constant. The current sensitivity of the galvanometer increases in direct proportion to the increase in flux level.

An example of the effect that air damping has on the current sensitivity of a practical long-period galvanometer can be seen by examining the Harris galvanometer. This unit has a current sensitivity of 2.90×10^{-10} A/mm at 1 m, at a free period of 110 sec and requires a circuit resistance of 1382 Ω for critical damping. The degree of air damping is 33.5% of critical. If the open-circuit damping were to be reduced by evacuating the air from around the moving system of the galvanometer, the flux level of the magnet would have to be increased to maintain the overall damping at its former value. In the case of the Harris galvanometer, evacuating the air and increasing the flux level would increase the sensitivity to 2.17×10^{-10} A/mm at 1 m, which represents an improvement of approximately 25%.

The reduction of air damping by evacuation is impractical with the usual moving-coil long-period galvanometer design such as the Harris galvanometer. The normal materials and methods of construction prevent extended operation at the relatively low pressures required. Tests on the Harris galvanometer have shown that air damping can be eliminated, for all practical purposes, at a pressure of 1×10^{-3} mm of mercury. At this pressure, various constituents of the materials used as cements, insulators, and encapsulants tend to boil off, and continuous pumping is required to maintain the vacuum.

If a vacuum is to be used to reduce the air damping of a galvanometer, the moving system must remain at the required low pressure. Thus, the materials enclosed in an evacuated chamber must have low vapor pressures and not tend to sublimate under vacuum conditions.

A possible solution to the problem of maintaining a vacuum around the moving system of the galvanometer is to reverse the normal positions of the coil and

magnetic assemblies. This arrangement places the magnet inside the evacuated housing with the suspensions. The magnet and the suspensions constitute the moving system. The coils, with their volatile constituents, are affixed to the outside of the housing. In this way, only materials adapted for use at low pressures are placed inside the housing, thus permitting the maintenance of the required vacuum for practical periods of time.

2.2 GALVANOMETER DESCRIPTION

2.2.1 General

Figures 1 and 2 are front and rear views of a long-period galvanometer designed to reduce air damping by operating the moving system in a vacuum. This instrument is designed to have free periods in the 100- to 200-sec range and to exhibit negligible air damping.

Figure 3 shows the outline dimensions of the galvanometer, as well as the arrangement of its various mechanical features. The rotor is composed of two ring magnets mounted on magnesium cups and separated by a turned magnesium mirror carrier. A fused-quartz mirror is mounted on the mirror carrier midway between the magnets. The rotor is supported, ideally, by quartz suspension fibers which are in turn supported at their outer end by spring housing assemblies. The moving system is enclosed in a Pyrex glass housing which is held in a vertical position by the mounting base. Two fixed-coil assemblies are mounted on the outer surface of the housing in close proximity to the ring magnets. A lens, mounted in an opening in the housing wall between the coil assemblies, focuses the light beam reflected from the mirror.

Light-spot adjustment is made by rotating the entire galvanometer relative to its mounting base. The moving system is locked for transportation by rotating the locking cap mounted at the top of the galvanometer.

2.2.2 Rotor Assembly

The moving-magnet configuration is susceptible to influence from stray external magnetic fields. Local magnetic fields, including the earth's field, modify the magnet position as well as the free period of the moving system. This influence can be reduced by the use of two astatically positioned magnets. At best, this relatively simple arrangement retains a substantial sensitivity to local magnetic disturbances.

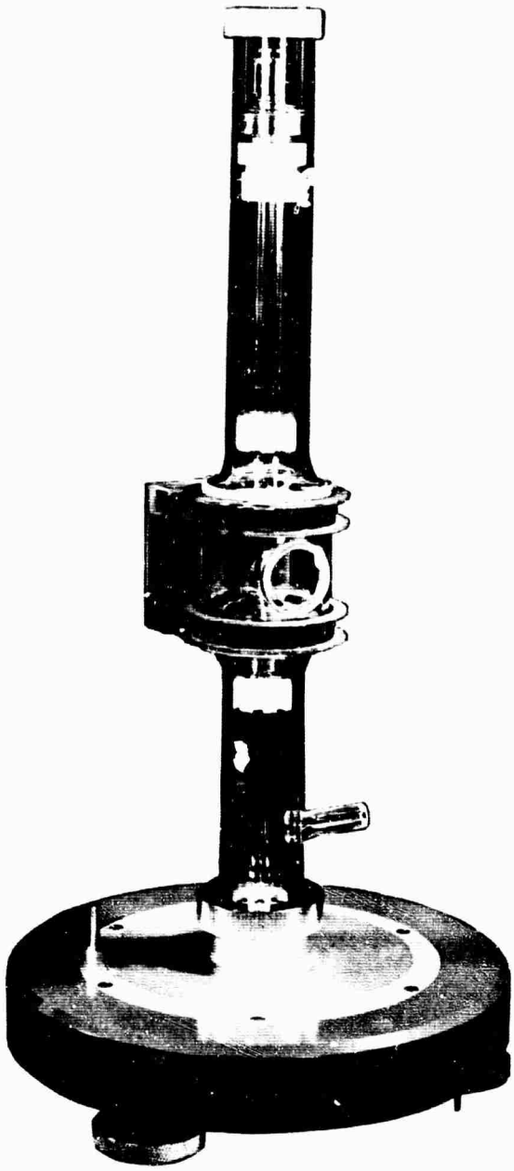

7599

Figure 1. Moving-magnet galvanometer, front view

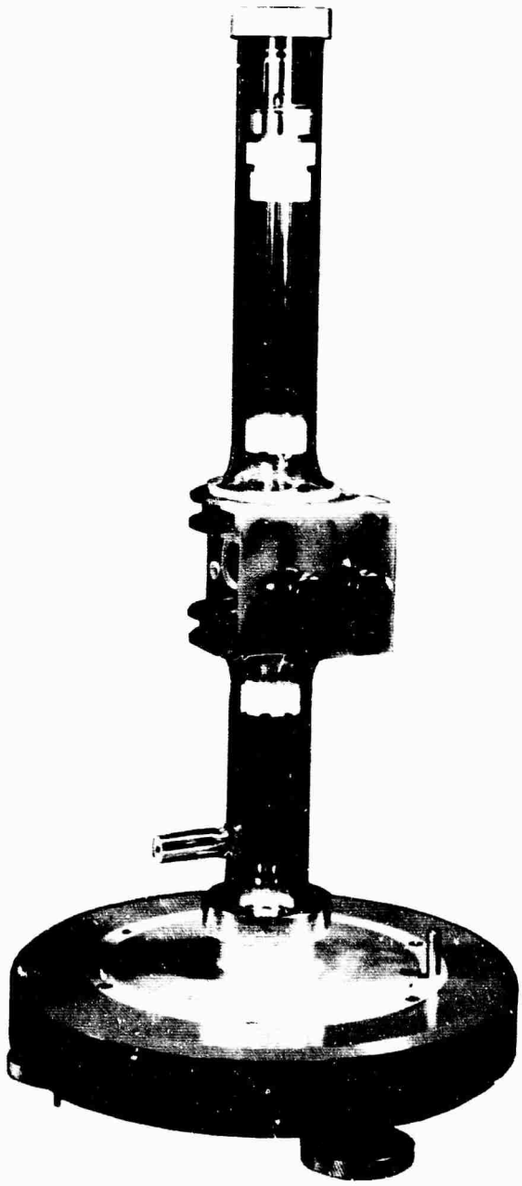

7600

Figure 2. Moving-magnet galvanometer, rear view

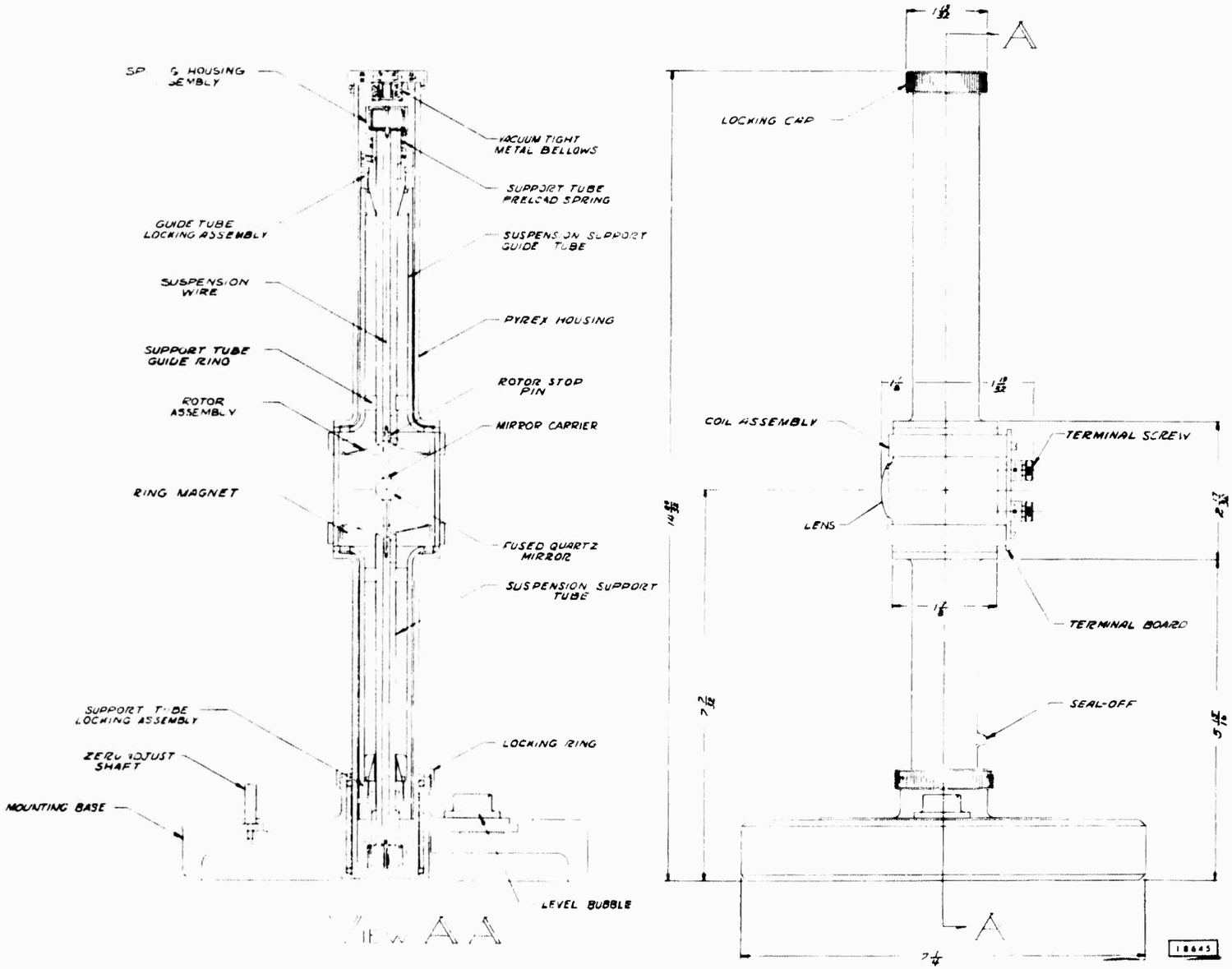

Figure 3. Galvanometer outline dimensions

A design which minimizes the response of moving magnets to magnetic disturbances is shown in figure 4. Instead of the four poles of the astatic arrangement suggested above several magnetic poles are used.

It is theorized that a sphere, with a large number of individual and identical magnetic poles evenly distributed over its surface, is least susceptible to influence from external magnetic fields. The rotor assembly shown in figure 4 approximates the spherical arrangement, in that the ring magnets are spaced to lie in the surface of a sphere.

Each ring has 16 magnetic poles of alternate polarities equally spaced around its circumference. At the time of rotor assembly, the rings are carefully oriented so that a north magnetic pole on the upper ring is positioned directly above a south pole on the lower ring and vice versa.

Figure 5 shows a Visi-Mag representation of the flux field resulting from a magnetized ring. This display was accomplished by distributing the Visi-Mag particles uniformly in a thin layer of silicone oil spread on the surface of a specially prepared plastic vessel.

2.2.3 Coil Assemblies

The motion of the suspended rotor is controlled by two coil assemblies. Each assembly has 16 separate coils arranged to encircle the ring magnets. The vertical conductors of adjacent coils are positioned in the flux field of the ring magnets and control the rotor position and electromagnetic damping. Figure 6 shows a coil assembly ready for mounting on the outside of the galvanometer housing.

Figure 7 shows the detailed relationship of the coils to the ring magnets, as well as some of the pertinent constants associated with them.

2.2.4 Galvanometer Linearity

Figure 8 is a plot of light-beam deflection versus current. Note that the rotor "locks-in" when the axis of a magnet pole on the rotor aligns with the axis of a coil. This lock-in occurs at 0.391 rad (22-1/2 deg) beam angle, which is equal to the angular spacing of the rotor poles and matching coils. At this deflection, a further increase in coil current will not result in increased rotor rotation.

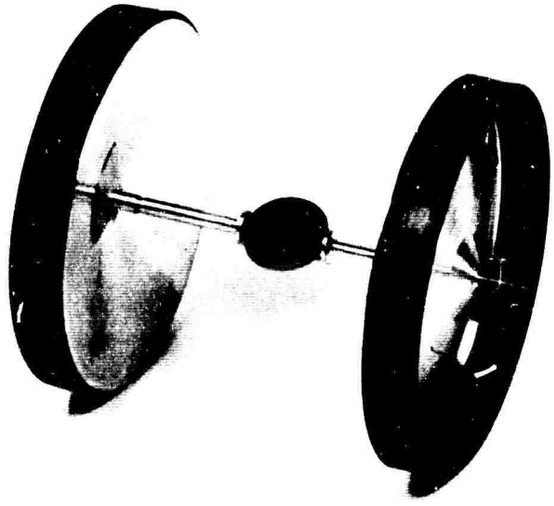

6118

Figure 4. Rotor assembly

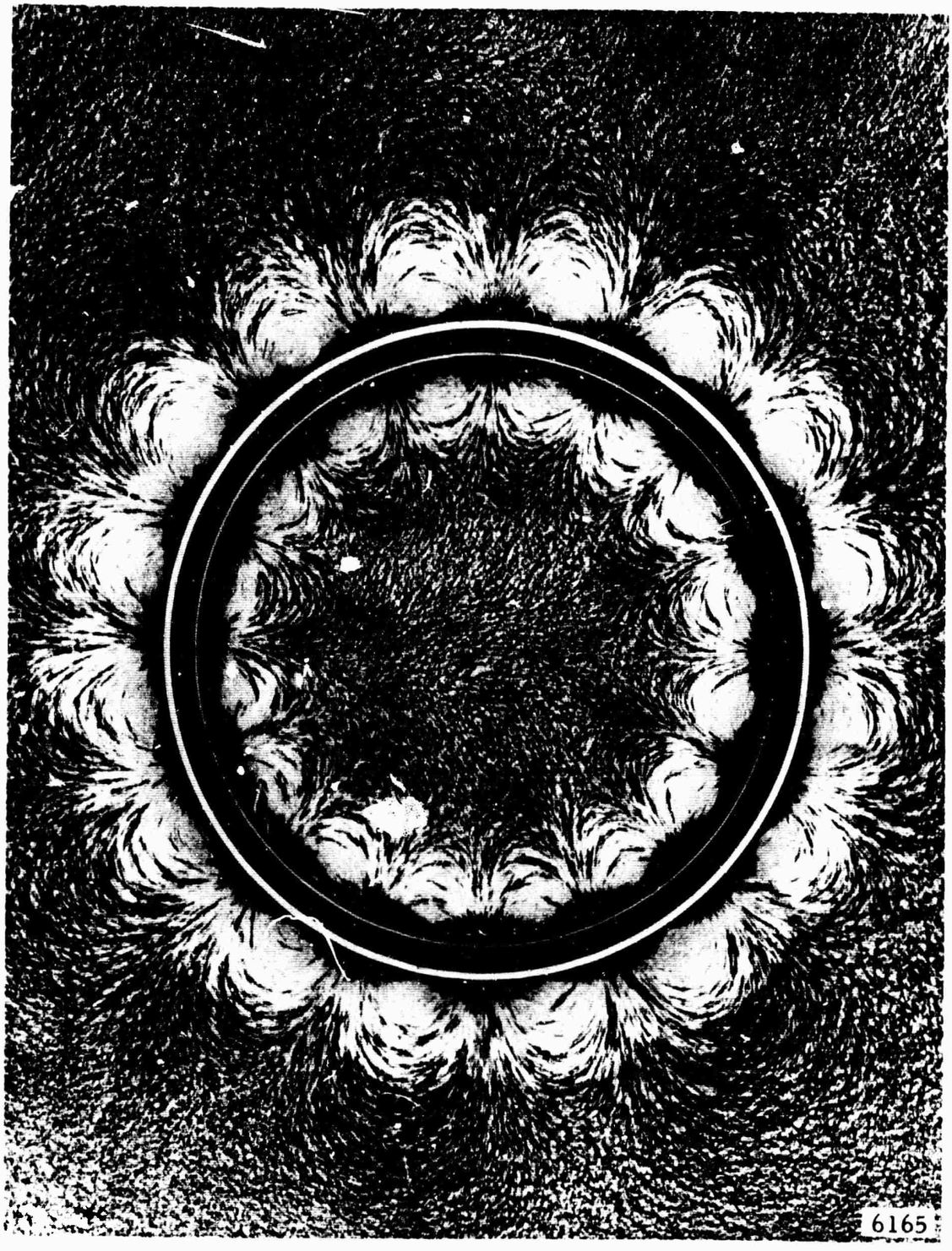

Figure 5. Visi-Mag representation of ring-magnet flux field

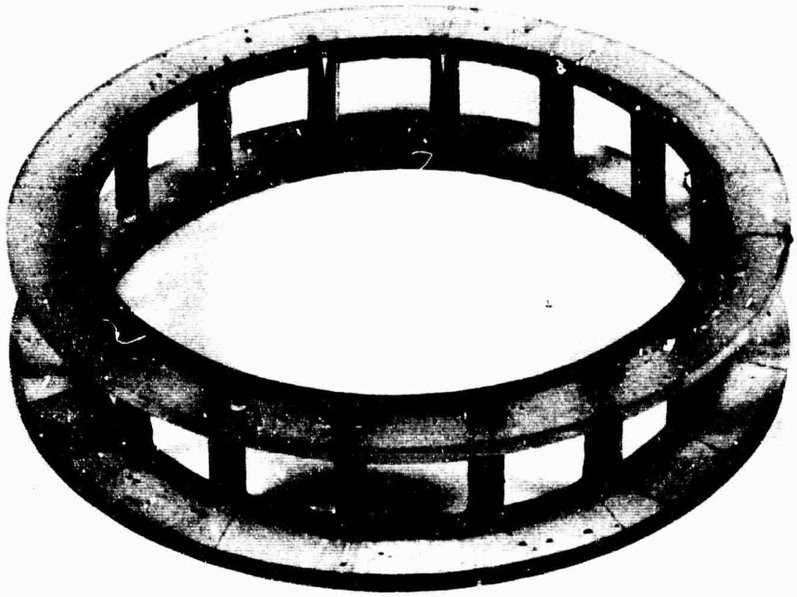

7123

Figure 6. Coil assembly

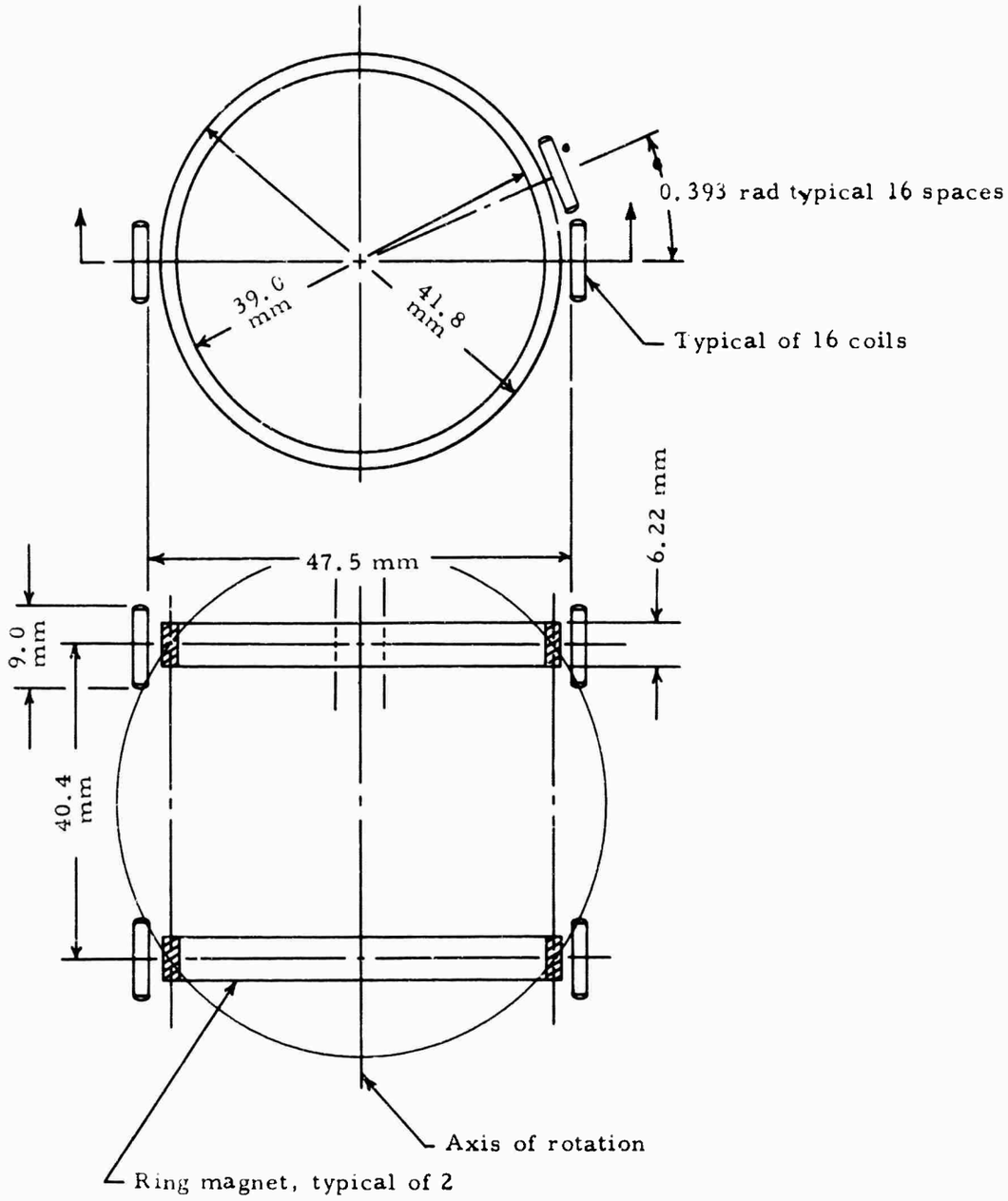

Material of ring magnet	Indox I
Weight of ring magnet (each of 2)	0.00482 kg
Moment of inertia of ring magnet (each of 2)	1.966×10^{-6} kg m^2
Flux density at coil plane (maximum)	0.0180 T
Number of turns per coil	155
Number of coils per assembly (2 assemblies required)	16
Total resistance per coil assembly	490 Ω

Figure 7. Relationship of coils to ring magnets

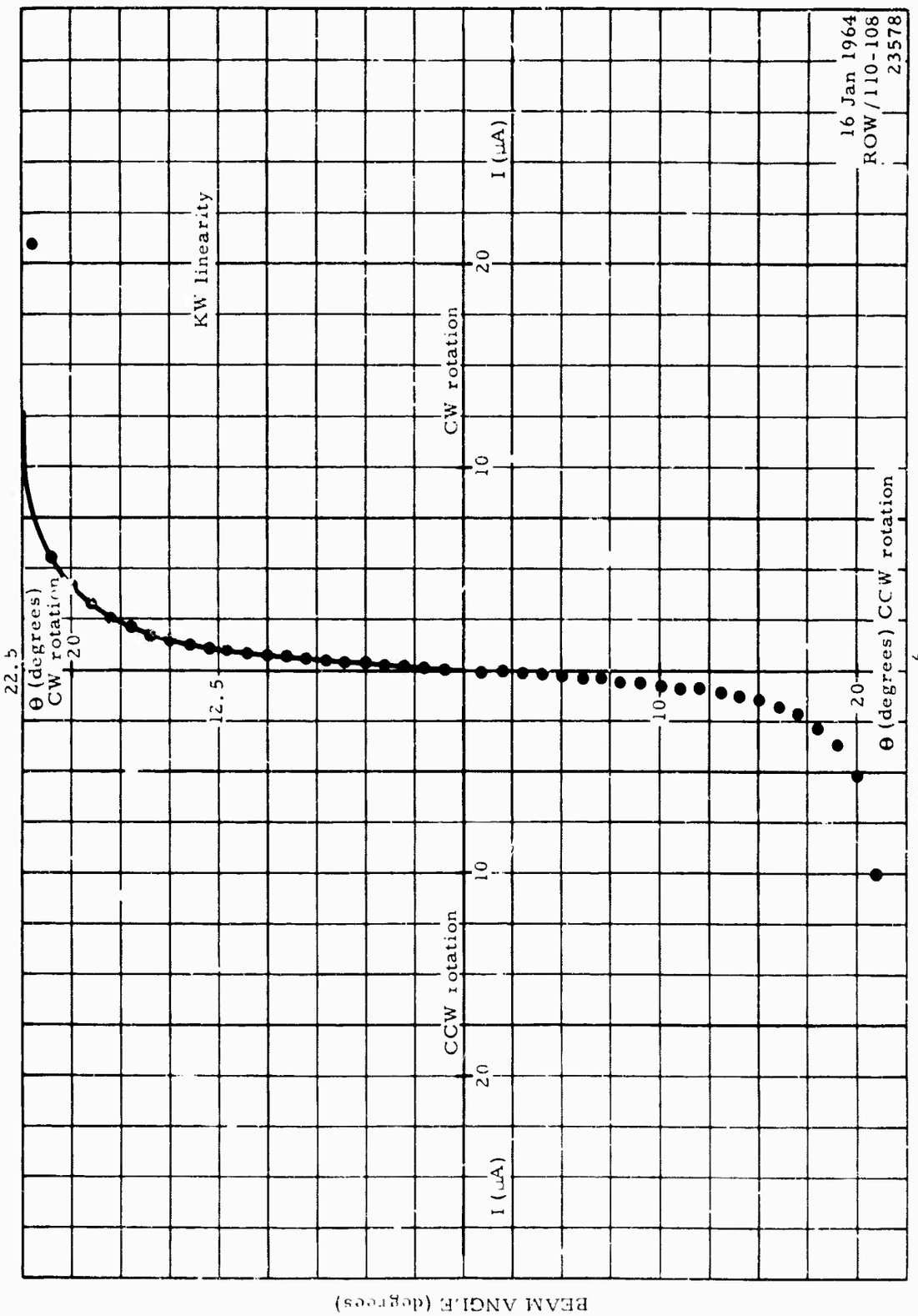

Figure 8. Light beam deflection versus normalized current

The system has limited linearity as demonstrated by figure 9. This figure is a plot of a portion of the data of figure 8 on an expanded scale. The light-beam linearity is essentially a straight-line function to ±0.087 rad (±5 deg) and is linear to within ±4% to ±0.174 rad (±10 deg). Beyond 0.174 rad, the deflection versus current falls off rapidly and reaches a limit at 0.39[illegible] rad (22-1/2 deg).

The galvanometer has been designed for use in Geotech's Model 5240 series of long-period phototube amplifiers. The optical system of these amplifiers will accommodate approximately 0.061 rad (3.5 deg) beam deflection before clipping. Since the linear range of the present galvanometer exceeds 0.061 rad, the design is considered acceptable for phototube amplifier use.

2.2.5 Ring-Magnet Flux Distribution

Figure 10 is a polar plot of the magnetic flux density at two selected distances from the ring-magnet periphery. The flux density was measured with a Hall-effect flux-meter probe rigidly held, with its sensitive axis aligned along the ring diameter. The ring was rotated relative to the probe with the aid of a fixture which indicated the angle in degrees. Thus, the normal component of flux was measured at each point. When comparing figure 10 with the Visi-Mag representation of the flux field of figure 5, note should be taken that the spatial relation of the two figures is reversed.

The values for the outer circle of plotting points were obtained with the probe in contact with the ring periphery. Although the absolute values of these readings are somewhat scattered, they tend to show a constant value of flux distributed over a relatively large angle. A close examination of figure 5 would suggest a relatively constant value of flux. The values for the inner circle of plotting points were obtained with the probe spaced at the coil-design distance from the magnet surface. This distance of approximately 2.4 mm (3/32 in.) is determined by the wall thickness of the glass housing plus the necessary dimensional clearance between the outside diameter of the magnet and inside diameter of the housing.

2.2.6 Extending Galvanometer Linearity

The linearity exhibited by the galvanometer (see figure 9), over and beyond the deflection required for phototube amplifier use, is not fully explained by the flux distribution as measured at the working distance (see figure 10). The linear range is extended by the vertical elements of adjacent coils spaced slightly apart. That is, as the magnet rotates through a small angle, the

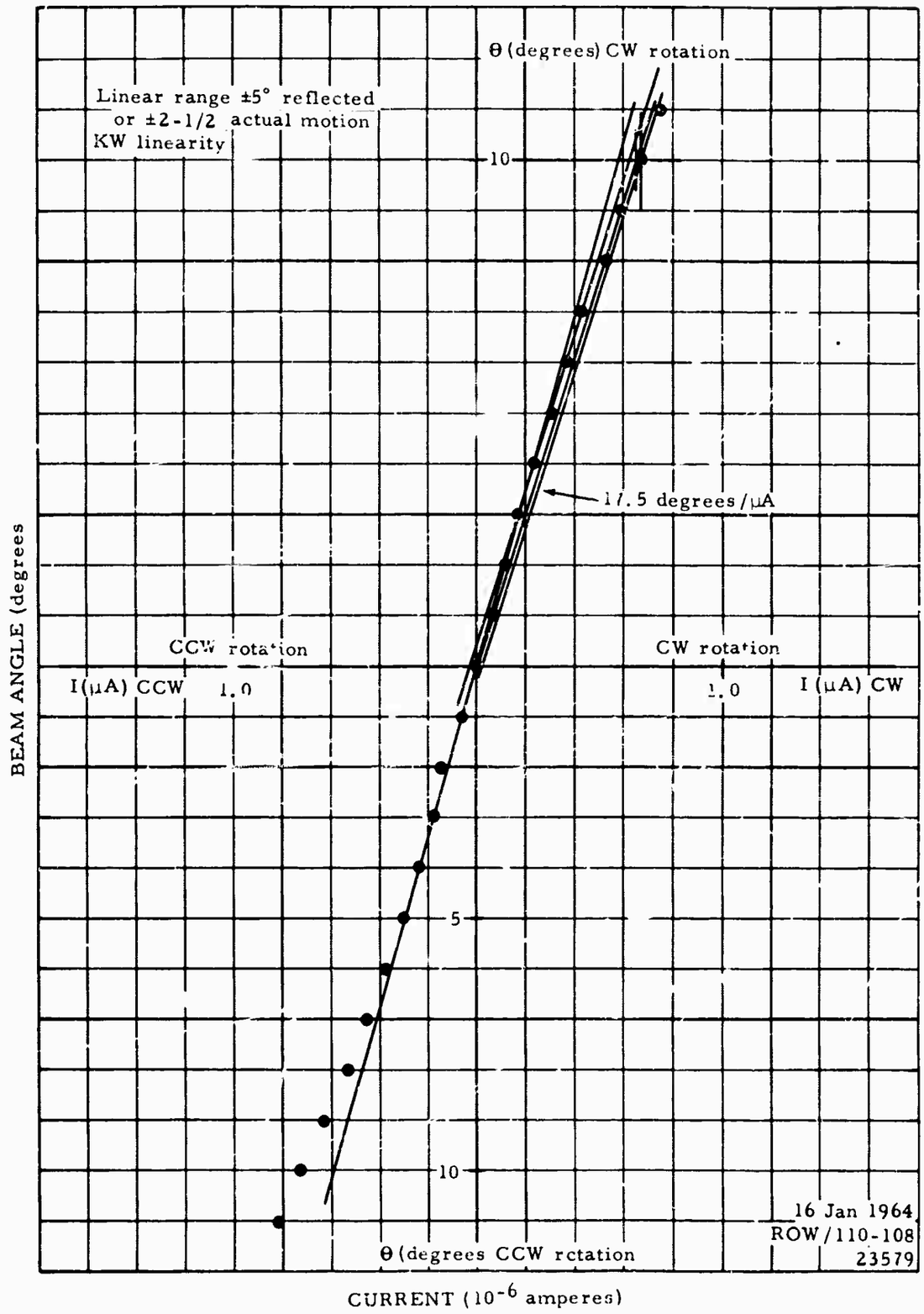

Figure 9. Light-beam deflection versus normalized current, expanded scale

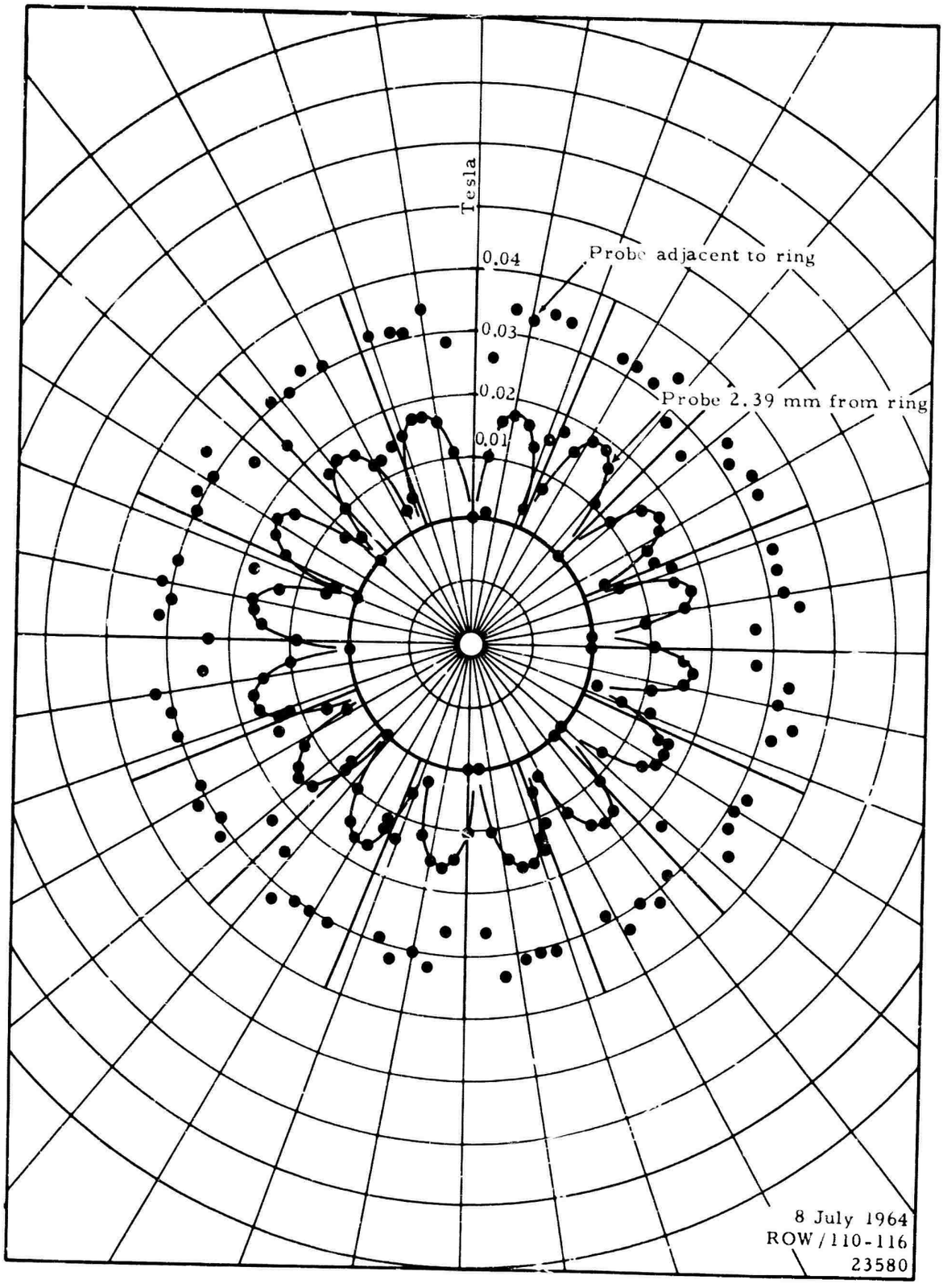

Figure 10. Ring magnet flux distribution, polar plot

vertical elements of one coil experience an increasing flux field while those of the adjacent coil experience a decreasing field. Thus, within limits, the vertical element spacing and/or wire distribution can be used to modify the linearity. The spacing used on the present instrument is not necessarily the spacing required for optimum linearity.

The angular relation of the top and bottom coil assemblies can also be used to extend the linearity of deflection versus current. The angular displacement of the two coils is accomplished by slightly rotating one coil relative to the other coil using the housing as an axis. The effect is the same as when the spacing of the vertical elements of adjacent coils is changed.

2.2.7 Material Selection Criteria

The rotor subjects the area immediately surrounding it to a magnetic field. This magnetic field would lead to undesired eddy current (electromagnetic) damping of the moving system, if the galvanometer housing and structures close to the rotor (other than the coils) were made of electrically conducting materials. For this reason, the housing is constructed of Pyrex brand glass tubing. The other materials in close proximity to the rotor are selected for similar reasons.

There is an additional criterion used in selecting the materials surrounding the moving system. The magnetic field of the rotor tends to magnetically polarize the materials surrounding it. After deflection, if the rotor remains "off zero," an element subject to the rotor's field has been magnetically polarized. In the case of some materials, this polarization will diminish with time as observed by a decrease in the rotor offset. With other materials, the polarization is essentially permanent, and unless it is modified by further rotor rotation in the same or opposite direction, it will continue to hold the rotor off zero.

The material used in encapsulating the coil assemblies is especially troublesome, and must be carefully selected for low magnetic susceptibility. Since it is desirable that the coil assemblies be self-supporting, a relatively rigid material is needed. In general, epoxies satisfy this requirement if selected with care.

Figure 6 shows the final coil assembly. The quantity of epoxy used has been minimized and was selected for its low magnetic susceptibility. The selection of a proper epoxy was made after testing approximately 25 samples supplied

by various manufacturers. Hysol brand (type H2-2038 base with type H2-3404 hardener) was chosen for giving the least zero offset and for having the desired mechanical properties.

2.2.8 High-Frequency Degaussing

The use of a selected epoxy as a coil encapsulant diminishes but does not entirely eliminate the polarization caused by the rotor's magnetic field. Even the use of a minimum quantity of Hysol H2-2038 epoxy (as shown in figure 6) results in detectable zero offset after rotor deflection. The effect of this polarization can be further reduced by introducing a high-frequency degaussing current into the signal coils. This current can be fed into the coils through capacitors connected across the coil terminals.

The application of a high-frequency degaussing current reduces the zero offset after rotor deflection and results in more dependable readings. Using a 40×10^3-Hz sinusoidal current, the zero offset was reduced to a minimum beam angle of 0.00166 rad (0.067 deg). In any given instance, the actual offset is dependent on the suspension restoring force, the ring magnetization level, and the rotor deflection angle used to initiate the offset. The offset (0.00166 rad) was obtained after a deflection of 0.391 rad (22-1/2 deg). Deflections within the linear range result in negligible offsets.

The use of high-frequency degaussing currents requires that no dc component be introduced into the galvanometer coils. This component can be largely avoided by using transformers or low-leakage capacitors for coupling and by avoiding rectifying contacts.

2.2.9 Suspension Material

Figure 11 shows the rotor in place in the inner housing. The figure shows the inner housing supported by a jig. The suspension fibers and various other parts are installed with the aid of this jig.

Considerable difficulty was encountered with the quartz fibers used to support the rotor. While satisfactory fibers of 0.025 mm (0.001 in.) in diameter can be drawn in quantity, (fibers with smaller diameters are drawn with difficulty). The biggest problem was the inconsistent breaking strength exhibited by the fibers at the working diameter of approximately 0.020 mm (0.0008 in.). An improvement in the breaking strength was made when an environment of pre-heated nitrogen was used to exclude the air from the region of the molten quartz. This technique tended to reduce the number of peripheral cracks,

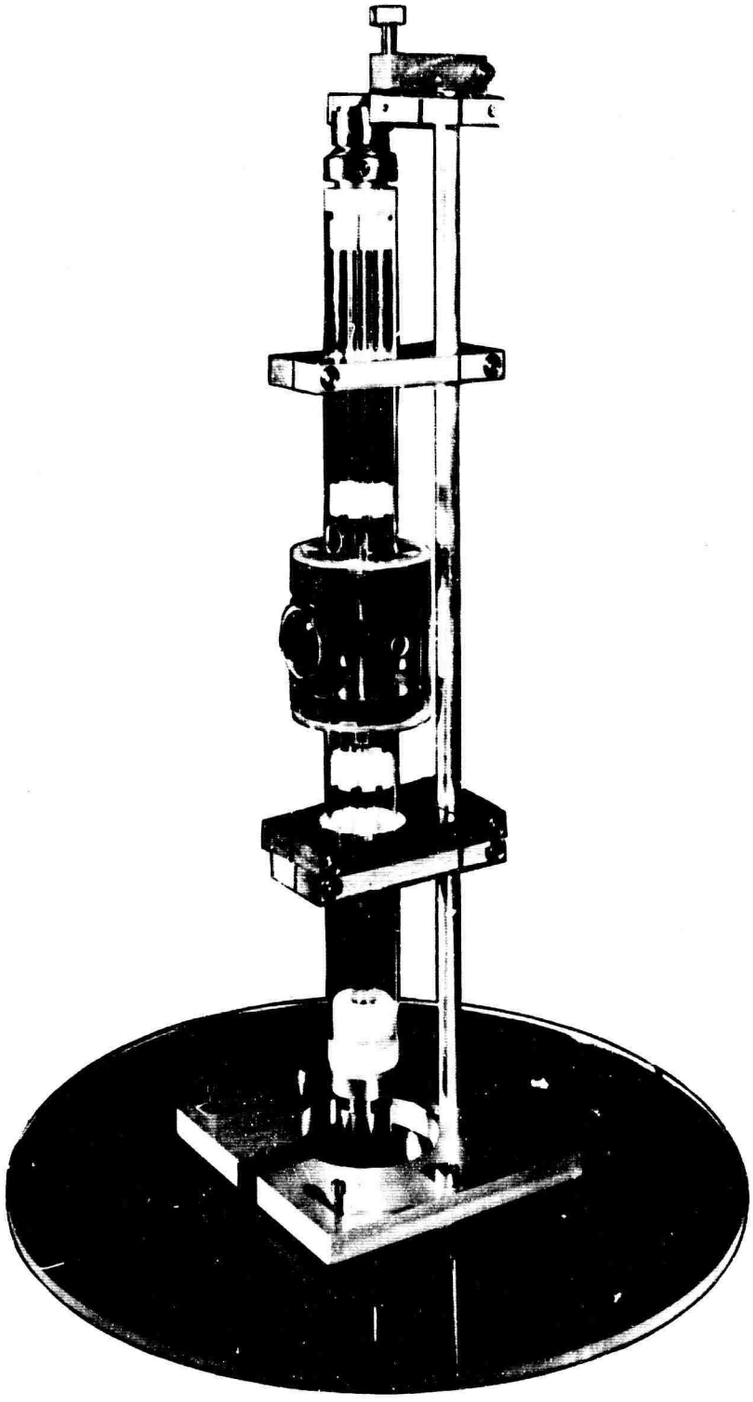

7764

Figure 11. Inner-housing assembly and support jig

which apparently result from too rapid cooling. Inclusion of foreign material in the melt was also reduced.

Although an improvement in strength was made and cleaner fibers were drawn by the improved method, the resulting fibers would not consistently support the rotor. Selected fibers of the same approximate diameter would support the rotor for random periods of several minutes to several days before breaking. It is clear that some sort of yield took place, possibly because of the minute peripheral cracks occasionally observed during fiber selection. It is assumed that in the fibers used, there were undetected cracks which contributed to the early failures.

The use of quartz fiber suspensions in the galvanometer, although desirable if losses are to be reduced to an absolute minimum, is not necessary for satisfactory operation. As the development project progressed, and it became increasingly evident that the successful use of quartz as a suspension material would require a great deal more time and effort than was available, a decision was made to use metal suspensions for the final test. The copper-silver alloy (94% Cu - 6% Ag) suspension wire used with the Harris galvanometer is readily available and was selected for use.

2.2.10 Galvanometer Optical System

Since the galvanometer is intended to operate in a Geotech Model 5240 long-period phototube amplifier, the optical system was designed with this in mind. A layout was made of the interior of the PTA to determine the focusing requirements of the system, the required lens aperture and the lens surface curvatures which would avoid spurious internal reflections or "ghosts." Focal lengths were obtained by ray-tracing techniques. An optical layout giving the lens characteristics is shown in figure 12.

2.3 TEST RESULTS

The following tests were performed at room temperature and under laboratory conditions.

The galvanometer was mounted on a concrete pier approximately 0.4 m from the nearest-magnetic material. The coil assemblies were connected in parallel for a total of 4944 effective turns. The terminal resistance in this configuration is 245 Ω.

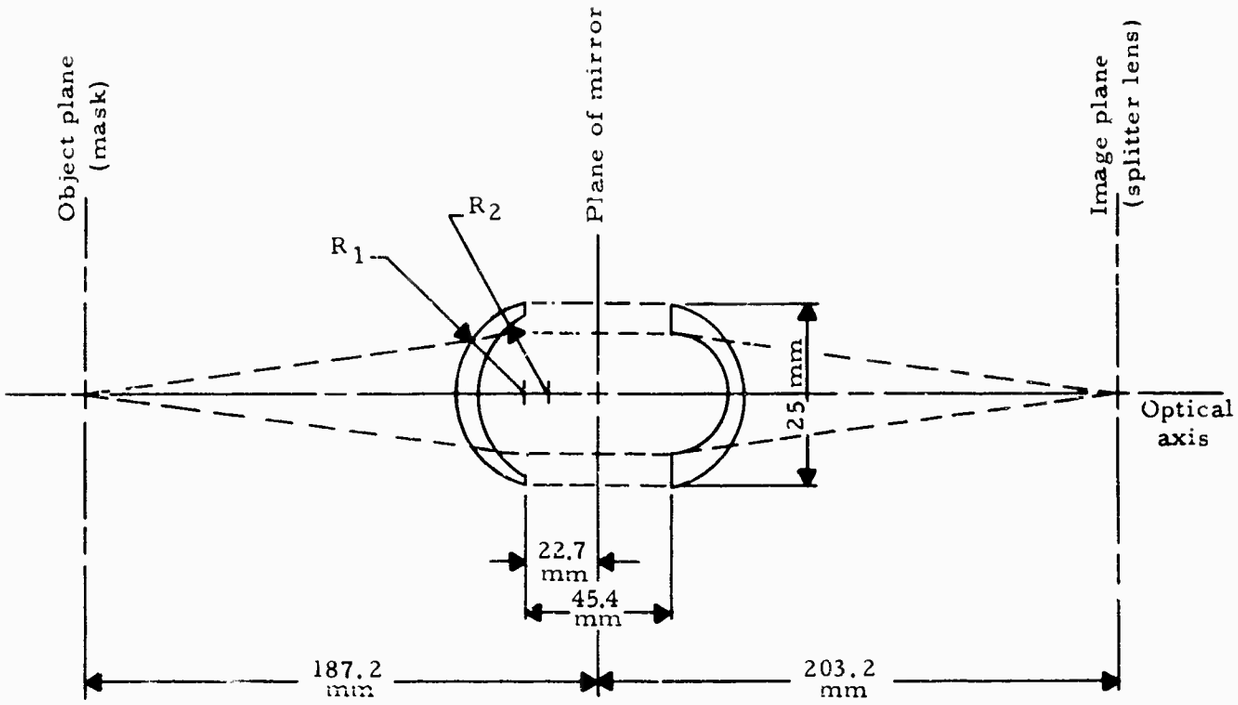

R_1 = 26.4 mm. R_2 = 37.2 mm
Lens material: No. 2 Borosilicate crown, N_a = 1.517
Lens focal length: 163.2 mm
System focal length: 97.4 mm

Note: Optical system shown unfolded for clarity. Actual system has only single lens.

Figure 12. Optical layout

The galvanometer was adjusted to vertical until the rotor would freely rotate without dragging on the housing. The rotor was allowed to seek its zero position as judged from the position of a light beam reflected from the rotor mirror. Since the total restoring torque of the moving system is the sum of the torque of the mechanical spring and the magnetic field (caused by the rotor magnetic unbalance), the initial rotor zero position did not coincide with the housing zero. To correct this, the housing was rotated to various magnetic headings until the two zeros almost coincided.

Final zero adjustment of the rotor was made by observing the current sensitivity for both left and right deflections and by observing the open-circuit damping decay. When symmetrical characteristics were obtained, for both left and right deflections, the galvanometer was assumed to be zeroed.

Once the zero position was established, the galvanometer was observed to be reasonably tolerant of magnetic heading and maintained essentially constant characteristics for ±0.262 rad (± 15 deg) beam angle on either side of the established zero position.

With the galvanometer at the zero heading, open-circuit damping, closed-circuit damping, and free-period tests were run at both room pressure and reduced pressure. The free period was measured at intervals during the deflection decrements, after a rotor release from 0.087-rad (5-deg) beam angle, for both left and right deflections. The period decreased slightly with decreasing deflection, from 71.4 sec at 0.087-rad (5-deg) amplitude to 70.3 sec at 0.017-rad (1-deg) amplitude, in a typical instance. The open-circuit damping ratio, as determined from the logarithmic decrement of deflection, is 0.050 at room pressure and decreases to 0.022 at a reduced pressure of 1×10^{-4} mm of mercury, which is a decrease of 56%.

It is reasonable to assume that evacuation of the air from around the moving system (ultimate pressure = 1×10^{-4} mm of mercury) did reduce the air pressure to a negligible value, and that the open-circuit damping after evacuation is due to other losses in the system. Possible causes of such losses are polarization of the epoxy which is used to encapsulate the coils and which is always in the magnetic field of the rotor, and frictional losses in the metal suspension used in the test unit.

Possible but unanticipated losses incurred through use of the high-frequency degaussing current were tested for by disconnecting the high-frequency leads to the galvanometer coils and repeating the period and damping tests. There was no detectable change in the damping characteristics with the current either on or off.

The total moment of inertia of the rotor is calculated to be 4.28×10^{-6} kg m^2. The measured spring constant is 3.14×10^{-9} Nm/rad. The calculated period, using these values of inertia and spring constant, is 232 sec. The observed period at small deflections is 70.3 sec.

Neglecting the small period correction for air damping (the period is always longer in the presence of air), the spring constant required to give a free period of 70.3 sec is 3.42×10^{-8} Nm/rad.

The restoring torque attributable to the magnetic spring is therefore:

$$(3.420-0.314)\,10^{-8} = 3.106 \times 10^{-8} \text{ Nm/rad},$$

or approximately a factor of 10 greater than the mechanical spring. This represents probably the maximum magnetic unbalance that can be expected, since appreciably better balance was achieved at earlier stages in the development.

The average damping ratio values of three tests are listed in the following table:

Test No.	Pressure	Average damping ratio	
		Open circuit	Short circuit
4	air	0.050	0.380
5	vacuum[1]	0.022	0.326
6	air	0.050	0.375

[1] 10^{-4} mm of Hg

From these data we can separate the total damping ratio into the sum of an air-damping ratio, an electrical-damping ratio, and residual-damping ratio:

$$\text{total} = \lambda\text{air} + \lambda\text{elec} + \lambda\text{resid.}$$

The air-damping ratio is the difference between the air and the vacuum test results:

$$\lambda\text{air (open circuit)} = 0.050 - 0.022 = 0.028$$

$$\lambda\text{air (short circuit)} = 0.377^{1} - 0.326 = 0.051$$

[1] Average of two observations

The difference in these values cannot be explained and 0.028 or 2.8% should be taken as the most reliable number since it is based on the greatest number

of observations. In a vacuum, the residual-damping ratio is 0.022. It is considered to be due largely to magnetic phenomena since a calculation of the damping ratio caused by frictional losses in the suspension wire yielded the number 0.0001. The electrical-damping ratio is the difference observed between open-circuit and short-circuit damping ratios:

$$\lambda \text{ elec} = 0.380 - 0.050 = 0.330$$

$$= 0.326 - 0.022 = 0.304$$

$$= 0.375 - 0.050 = 0.325$$

$$\text{or } \lambda \text{ elec} = 0.320 \text{ average} = 32.0\% \text{ of critical}$$

This value is reasonably close to a predicted electrical-damping ratio of 0.492 which was based on an effective flux density of 0.01 T and a period of 70 sec.

The following is a summary of the characteristics of the test galvanometer:

Free period (room pressure)	70.5 sec (small deflection)
Free period (reduced pressure = 10^{-4} mm of Hg)	70.2 ec (small deflection)
Moment of inertia of rotor (calculated)	4.28×10^{-6} kg m^2
Spring constant (mechanical)	3.14×10^{-9} Nm/rad
Spring constant (calculated from period and inertia)	3.42×10^{-8} Nm/rad
Magnetic spring (attributed to rotor magnetic unbalance)	3.106×10^{-8} Nm/rad
Weight of rotor	0.0122 kg
Material of rotor	Indox I
Density of ring magnets	4.392×10^{-3} kg/m^3
Weight of ring magnets (each of two)	0.00482 kg

Measured flux density at surface of ring magnet (average)	0.032 T
Measured flux density at working distance (maximum)	0.018 T
Number of magnetic poles (each ring magnet)	16
Single pole area (at surface of ring magnet)	0.510×10^{-4} m^2
Number of coils (each of two assemblies)	16
Number of turns per coil	155
Number of turns per coil assembly	2472
Terminal resistance (each of two coils)	490 Ω
Active conductor length (single vertical element)	9 mm
Current sensitivity (parallel coil connection)	2.46×10^{-9} A/min at 1 m
Open-circuit damping (room pressure)	5.0% of critical
Open-circuit damping (reduced pressure = 10^{-4} mm of Hg)	2.2% of critical
Closed-circuit damping (room pressure, parallel coil connection, circuit resistance = 245 Ω)	37.5% of critical
Closed-circuit damping (reduced pressure = 10^{-4} mm of Hg, parallel coil connection, circuit resistance = 245 Ω)	32.6% of critical
Focal length of galvanometer	99 mm
Diameter of mirror	9.5 mm
Physical characteristics	
Height	0.38 m (15 in.)
Diameter	0.184 m (7-1/4 in.)
Weight	1.99 kg (4.38 lb)

2.4 CONCLUSIONS AND RECOMMENDATIONS

A moving-magnet, long-period galvanometer has been successfully constructed which has reduced damping when the air surrounding the moving system is evacuated. The galvanometer has not been fully tested, but preliminary tests indicate that the open-circuit damping has been reduced by 56% at a free period of 70.3 sec. This reduction is less than that expected and is thought to be explained by losses in the system other than air damping.

The galvanometer is considered to be of practical use only where its unusual design features may be of value. In its present stage of development, the galvanometer is difficult to construct and adjust, and at this time, is recommended for use as a laboratory instrument only.

There are three areas where improvement is indicated. A better rotor magnetic balance is required; the losses other than air damping should be reduced; and the percent of electromagnetic damping should be increased.

The best rotor magnetic balance that was achieved did not leave the rotor sufficiently astatic. The characteristics of the galvanometer are thus determined, to a large degree, by the local magnetic field. Because of this, the galvanometer must be oriented to an appropriate magnetic heading for proper operation.

The unexpected losses observed after galvanometer evacuation are thought to be caused by magnetic polarization of the epoxy used to encapsulate the coils and frictional loss in the metal suspension wire used in the test unit. In either case, energy is extracted from the moving system and damping results.

The percent of electromagnetic damping observed at the test unit free period of 70.3 sec is 32% for a circuit resistance of 245 Ω. This is not a useful percentage of damping and circuit resistance, and both need to be increased. Since the maximum flux level in the moving-magnet configuration is determined largely by considerations other than damping, an increase in the electromagnetic damping is most readily made by increasing the period.

The basic design features of the moving-magnet galvanometer, such as the vacuum-tight housing, housing support system, suspension support system, and the rotor locking details are directly applicable to the torsion pendulum of Task 1j, Investigation of Thermal Noise, and have so been used.

It is recommended that further development of the moving-magnet galvanometer be undertaken on a low-priority basis, possibly in conjunction with the torsional pendulums of the thermal noise investigation.

3. POWER LEVEL GALVANOMETER

3.1 GENERAL

A computing or dynamometer-type galvanometer has been constructed and tested for use in seismic data analysis. It is intended for use with Geotech Model 16956 photocell amplifiers. The sensitivity of the computing galvanometer is less than that of conventional units using permanent magnet fields and must be fluid damped.

Expected applications are signal squaring, with the fixed and moving coils connected in series and the output indicating power level, and multiplication with a separate input to each coil. When used with low-speed magnetic-tape transport, continuous signal comparison is possible.

3.2 DEVELOPMENT

3.2.1 Design Objectives

The physical dimensions of the computing galvanometer were determined by the dimensions of the Model 16956 photocell amplifier. Therefore, the computing galvanometer is the same size and shape as the Model 16259 short-period galvanometer already used in the PCA. The PCA was modified so that the galvanometer field coils could be driven by a separate input amplifier.

Since the unit is not required to damp itself, the choice of coil resistances was not limited by the usual galvanometer design considerations. The galvanometer was designed to have an apparent resonant frequency of 8.2 Hz and a damping ratio of 0.7 with fluid damping.

3.2.2 Description

3.2.2.1 General Physical Data

The Model 11570 computing galvanometer uses the same outer case as the Model 16259 short-period galvanometer. The computing galvanometer is shown in figure 13 and mounted in a Model 16956 photocell amplifier in figure 14. Galvanometer dimensions are shown in figure 15.

Figure 16 is an exploded view of the computing galvanometer showing its parts and their relationship. The suspension assembly is identical to that of the Model 16259-20 short-period galvanometer except that the magnet pole pieces have been replaced with a pair of field coils, as shown in figure 17.

The four terminals are located on the rear of the galvanometer (see figure 13). The horizontal pair is the fixed-coil input and vertical pair is the moving-coil input.

3.2.2.2 Suspension Assembly

The moving coil is wound with 33.5 turns of AWG No. 50 copper wire and is suspended by a pair of flat gold ribbons with a torsional spring constant of 0.21×10^{-9} Nm/rad/m. The nominal resistance of the assembly is 29.0 Ω and the resonant frequency is 20.0 Hz in air. It is mounted in a temperature-compensated frame which is also used in the Model 16259 series of short-period galvanometers.

3.2.2.3 Field Coils

The two fixed coils may be seen in place on the suspension frame in figure 17. Each coil has 11,780 turns of AWG No. 42 copper wire. They are connected in series and have a resistance of 9,800 Ω. They will produce a flux density of 53 T/A.

3.2.2.4 Fluid Damping

Because the flux density produced by the field coils is quite low when compared to that produced by the permanent magnets in a conventional galvanometer, the computing galvanometer cannot be electromagnetically damped. Instead, it operates in a silicone fluid which provides viscous damping. A fluid with an approximate viscosity of 2.044×10^{-5} m^2/sec and a density of 955 kg/m^3 lowered the natural frequency to 8.2 Hz and gave overshoot characteristics that indicated a damping ratio of 0.70.

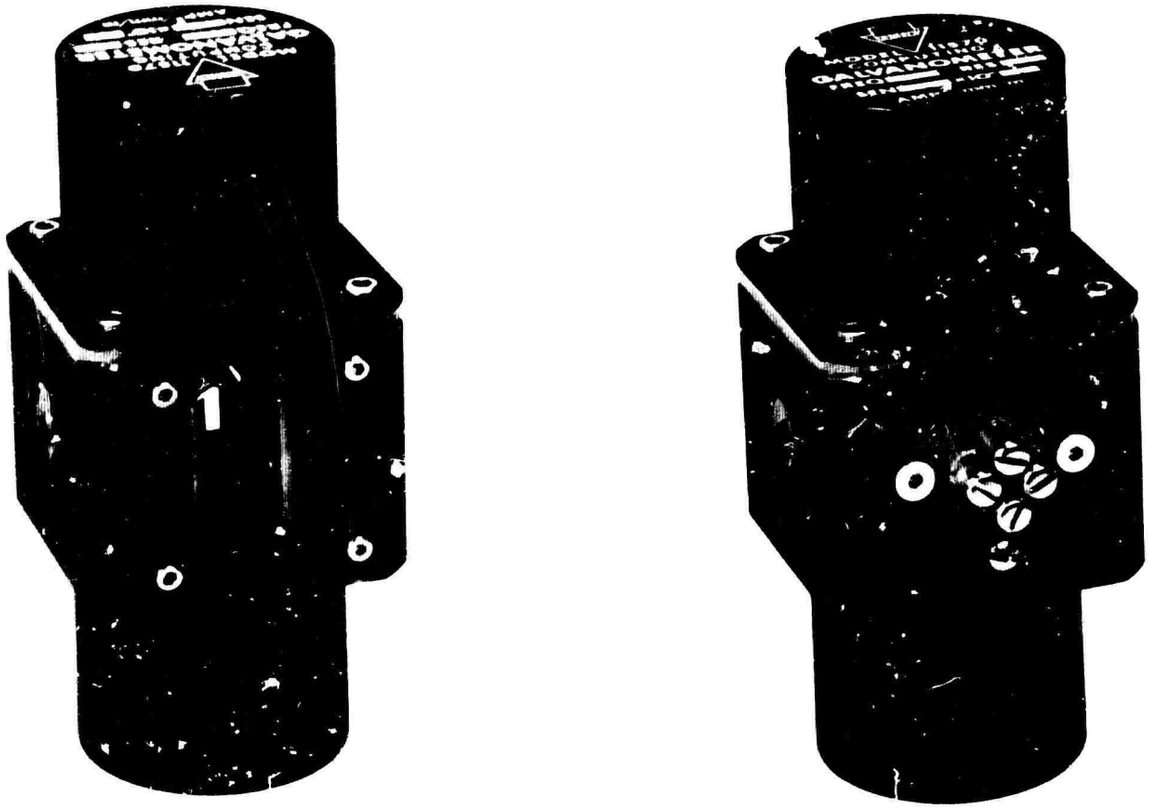

7618 7619

Figure 13. Computing galvanometer

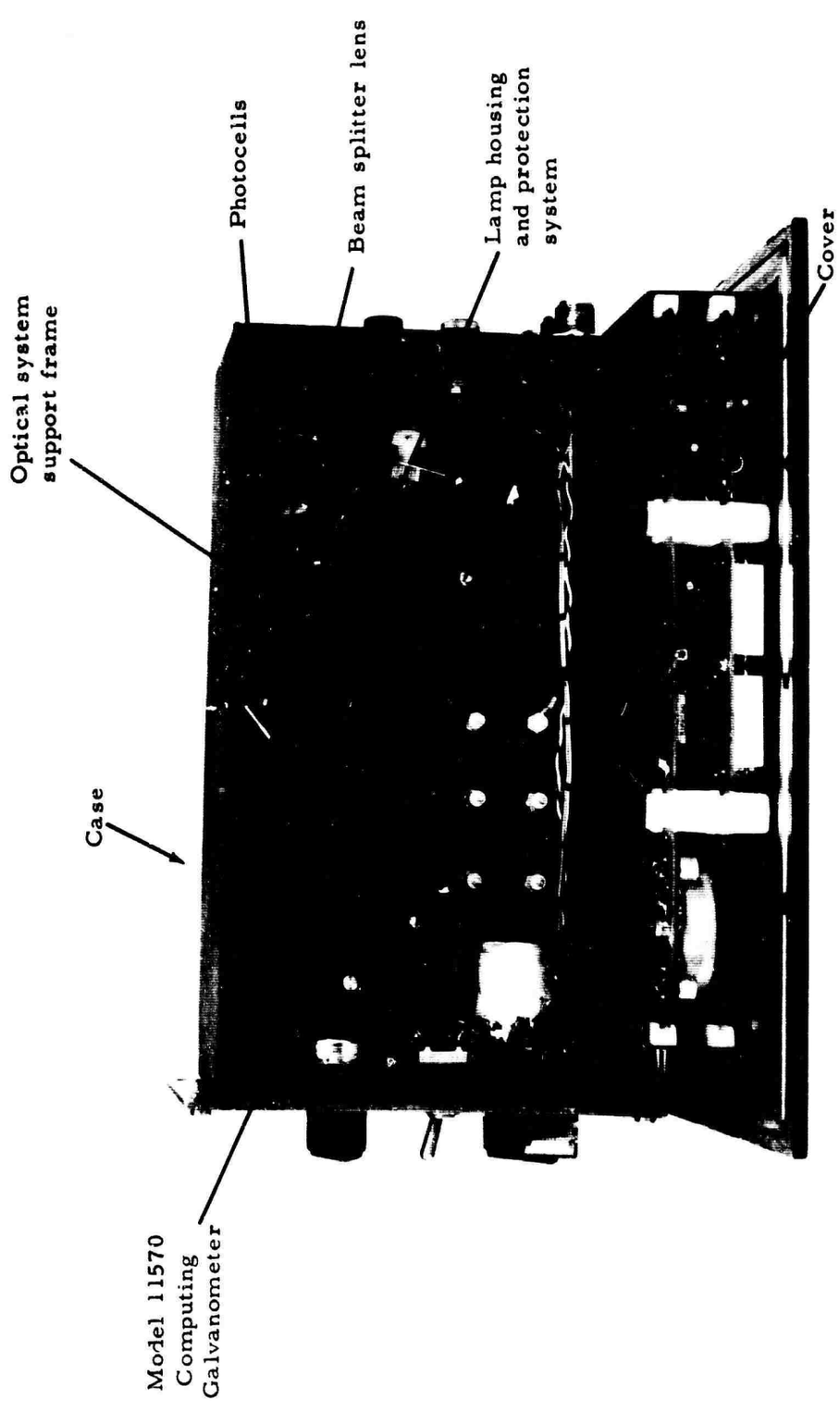

7078

Figure 14. Photocell amplifier, side view with case open

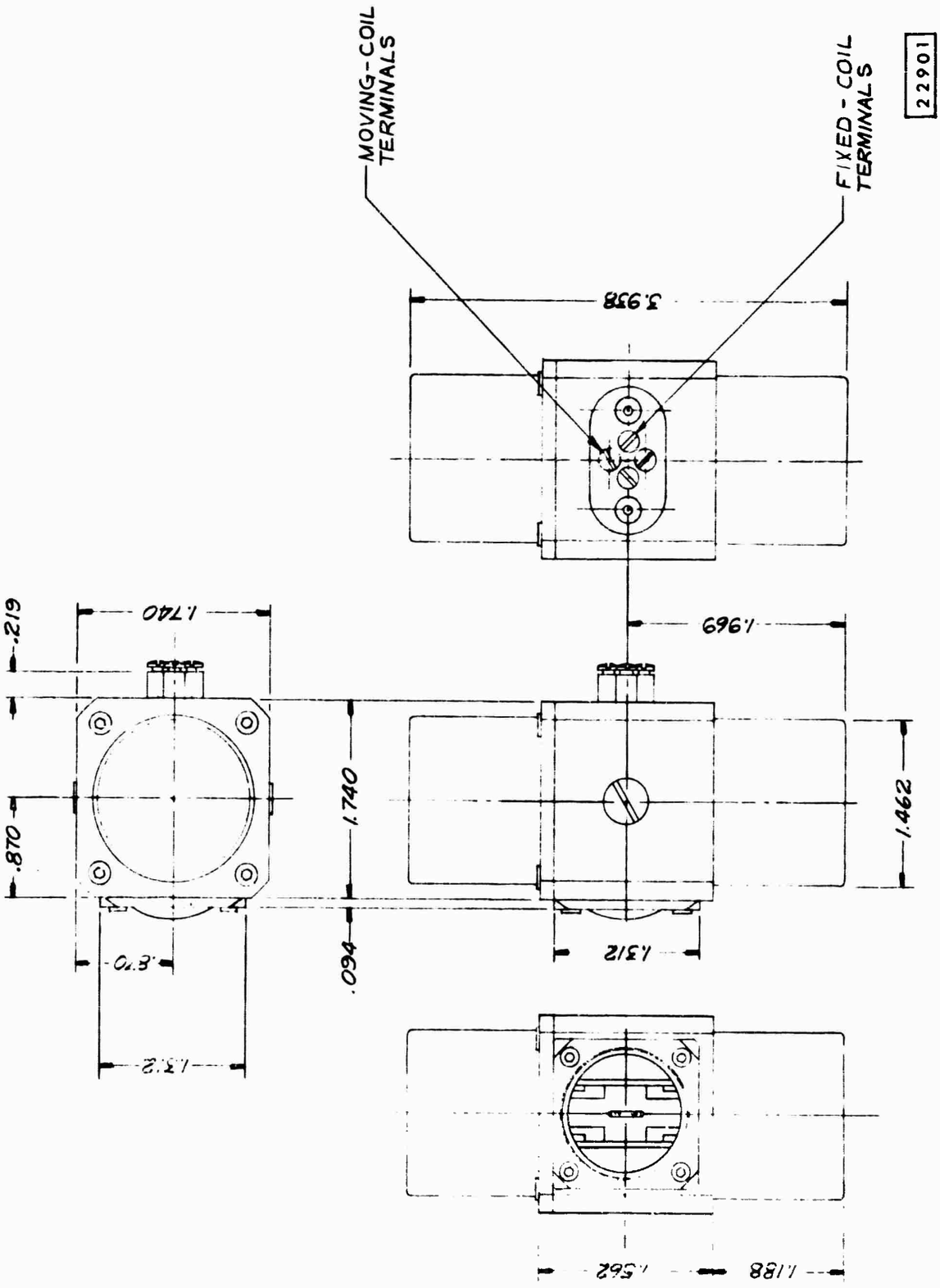

Figure 15. Computing-galvanometer outline dimensions

7604

Figure 16. Exploded view of computing galvanometer

7605 7606

Figure 17. Computing-galvanometer suspension frame and field coil assembly, front and rear views

3.2.2.5 Balancing

Since the suspension is submerged in a fluid, both mass and volume adjustments must be made. This is a tedious procedure because the balance observation must be made with the suspension in fluid and the required adjustment made with the suspension dry and in air. The mass balance is adjusted by adding solid glass beads to the coil assembly. The volume balance is adjusted by using hollow glass spheres.

3.2.2.6 Optics

The lens design is unusual for galvanometers and had to allow for the fact that the space between the lens and the mirror was filled with silicone fluid with a refractive index of 1.400. Object and image distances were obtained from a photocell amplifier layout, and ray-tracing techniques were used in the lens design. The final divergent meniscus lens has an aperture of 31.5 mm and a 125-mm focal length in silicone fluid as shown in figure 18. It is interesting to note that the lens is divergent in air but that the system is convergent due to refraction at the lens-fluid interface.

3.3 TEST RESULTS

3.3.1 Frequency Response

As previously stated, the undamped resonant frequency of the suspension in air is 20 Hz. In fluid, the resonant frequency is lowered because of an increase in the suspension moment of inertia caused by the fluid. Because the velocity-generated voltage in the coil was too small to measure directly, another method of finding the resonant frequency of the suspension in fluid had to be used. The viscosity of the fluid was first selected to provide the proper step-function overshoot for a damping ratio of 0.70. The steady-state sine-wave amplitude response for the frequency range of 0.8 to 80.0 Hz was then recorded. The resonant frequency in fluid was that value which (when used as a normalizing factor) allowed the normalized amplitude response data to fit the general normalized second-order response curve for a damping rate of 0.70. The result is shown in figure 19.

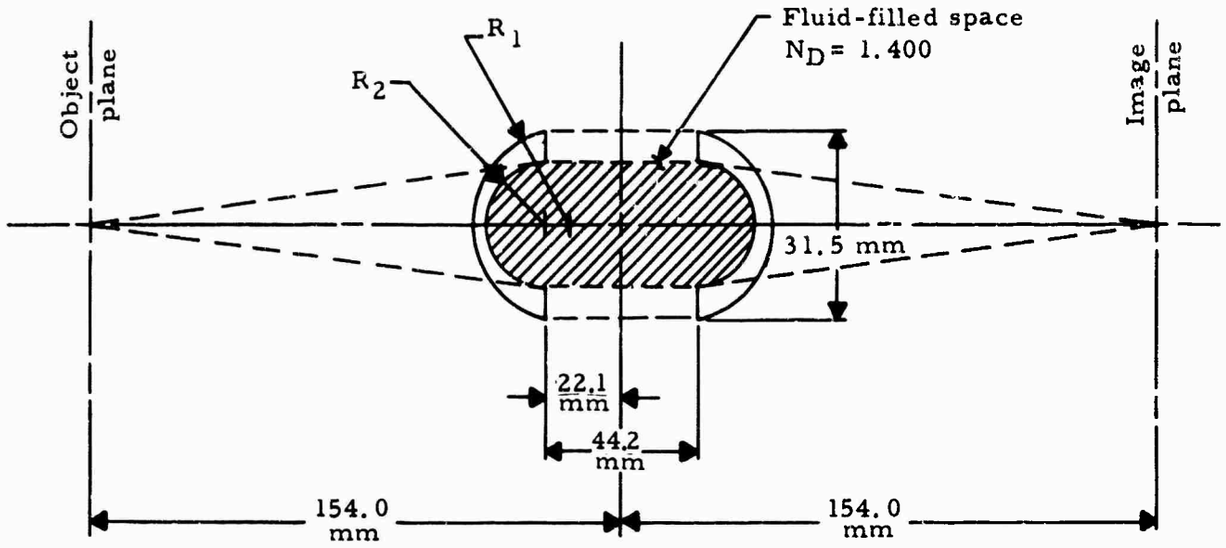

R_1 = 34.1 mm, R_2 = 27.4 mm
Lens material: No. 2 Borosilicate crown, N_D = 1.517
Lens focal length: 296.1 mm in air
System focal length: 77.0 mm

Note: Optical system is shown unfolded for clarity. Actual system has only single lens.

Figure 18. Computing-galvanometer lens

3.3.2 Operationsl Tests

3.3.2.1 Sine-Wave Input, Series Conne tion

Figure 20 is a tracing of a Visicorder record of the comp'ıting-galvanometer's sine-wave response with the coils connected in series. Note that the output signal is doubled in frequency compared to the input signal. The squaring capability of the galvanometer is illustrated in figure 20. As the amplitude of the input signal is increased by a factor of 2, the amplitude of the output signal is increased by a factor of 4.

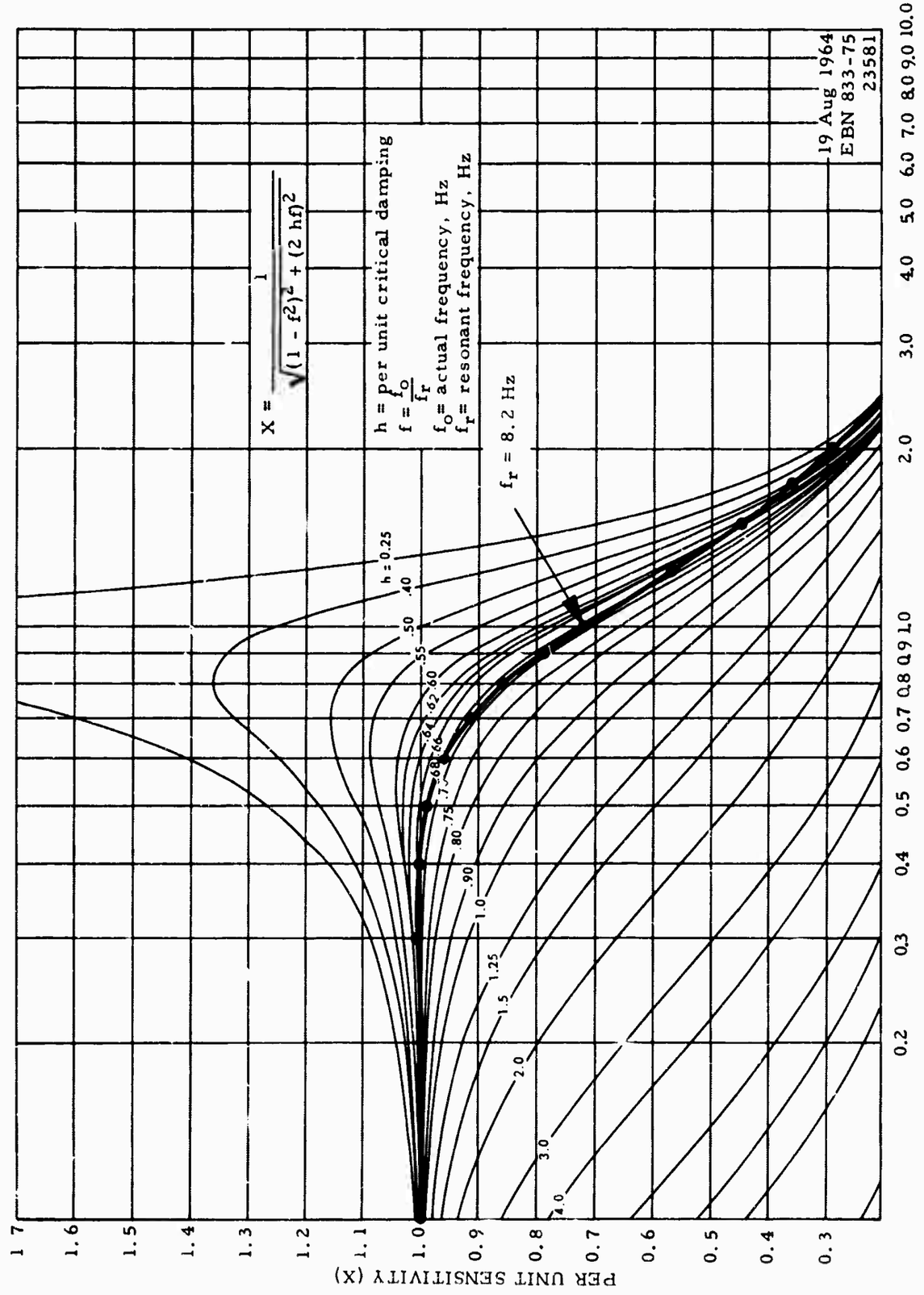

Figure 19. Comparison of galvanometer frequency response

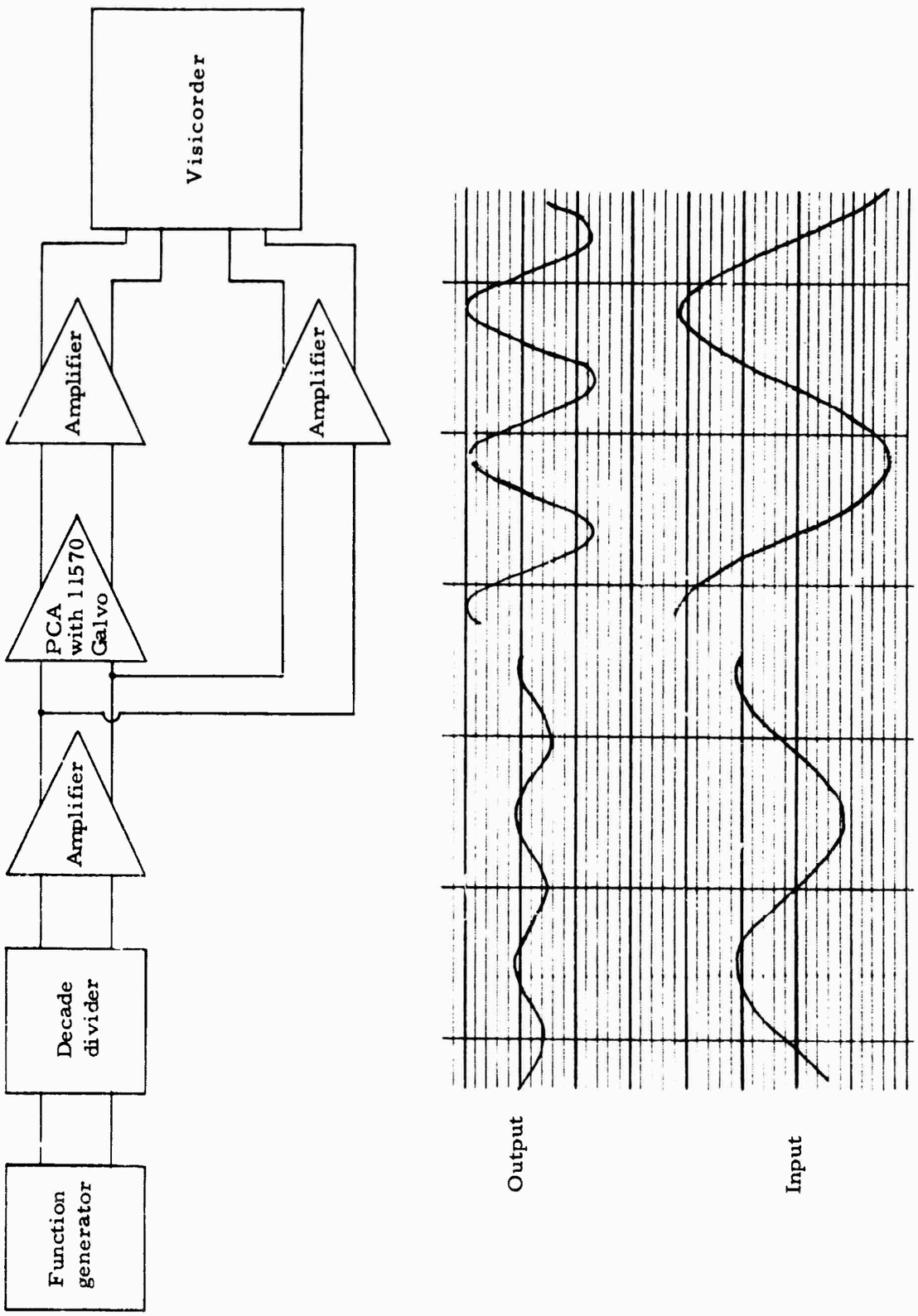

Figure 20. Tracing of Visicorder record, computing-galvanometer response to sine-wave input, series coil connection

3.3.2.2 Seismic Signal Input, Series Connection

Figure 21 is a tracing of selected portions of a Visicorder record of the response of the computing galvanometer to input from a magnetic-tape recording of an earthquake. The coils are connected in series.

The upper trace is the computing-galvanometer output and is proportional to the power in the original signal. Note that the signal is rectified, and lies on one side of the base line. The slight overshoot of the base line during the first few cycles is caused by the PCA filter time constant.

The lower trace shown on figure 21 is a standard analog recording of the magnetic-tape playback and was made simultaneously with the power trace.

3.3.2.3 Seismic Signal Input, Multiplication Connection

Figure 22 is a tracing of selected portions of a Visicorder record of the response of the computing galvanometer to a known event (Hard Hat) with the coils connected for multiplication. The magnetic-tape playback of the vertical seismic component was applied to the galvanometer suspension (moving coil). The horizontal component was applied to the field coils (fixed coils). In the figure, both the analog playback of the vertical and horizontal components are recorded along with galvanometer output.

The following is a summary of the characteristics of the computing galvanometer:

Moving coil	
Number of turns	33.5
Wire size	AWG No. 50 (32.8 Ω/m)
Terminal resistance (includes suspension ribbons)	29.0 Ω
Fixed coils	
Number of turns (each of two coils)	11,780
Wire size	AWG No. 42 (5.61 Ω/m)
Resistance (each of two coils)	4,900 Ω
Terminal resistance (two coils in series)	9,800 Ω
Rating (flux density between series connected coils)	53 T/A

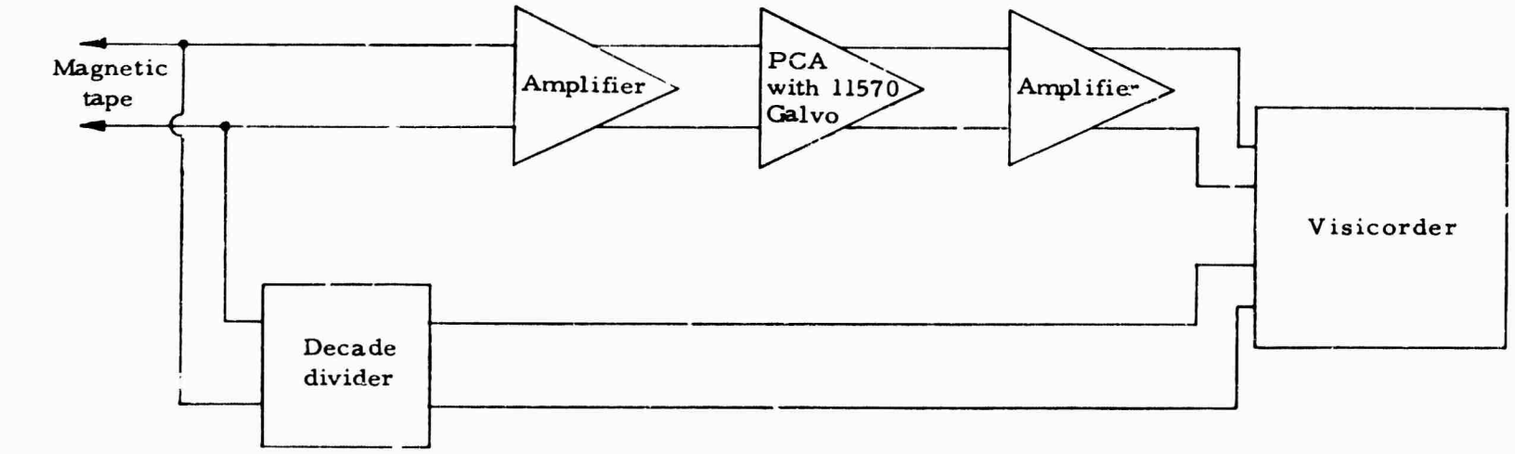

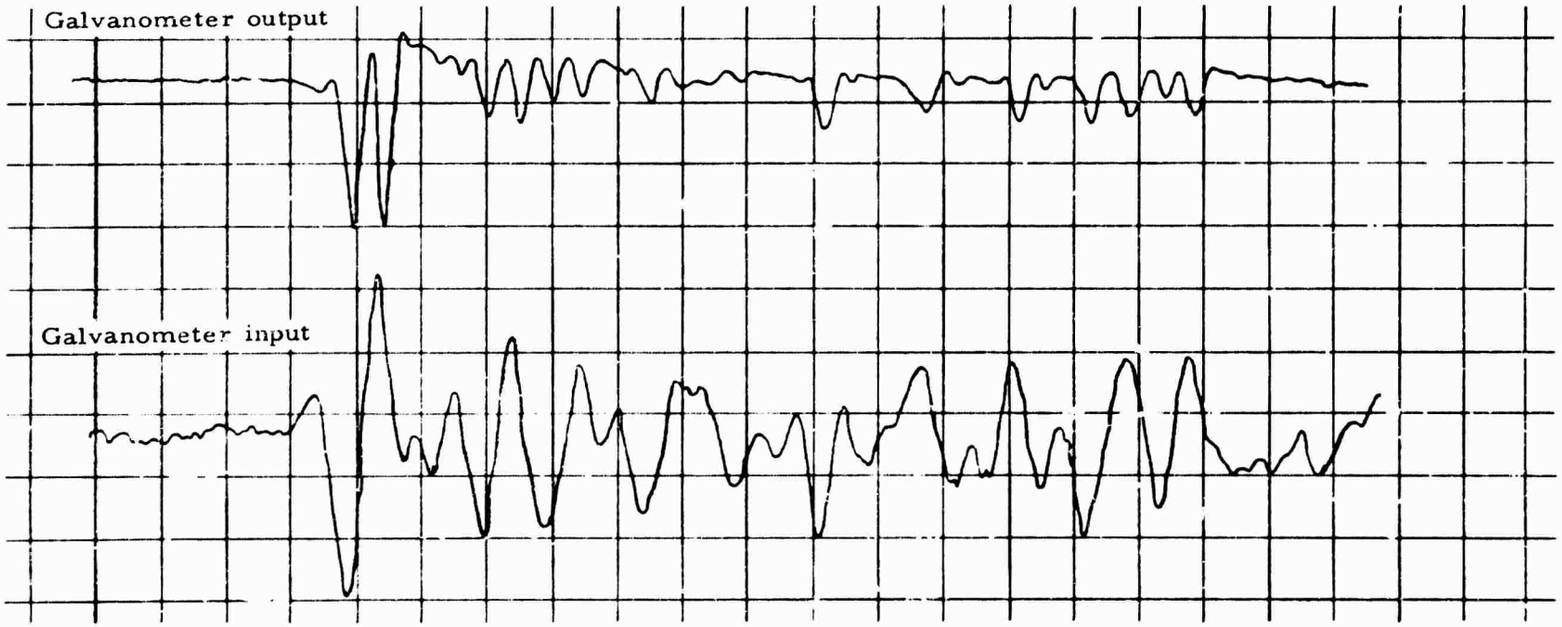

Figure 21. Tracing of Visicorder record, computing-galvanometer response to earthquake input, series coil connection

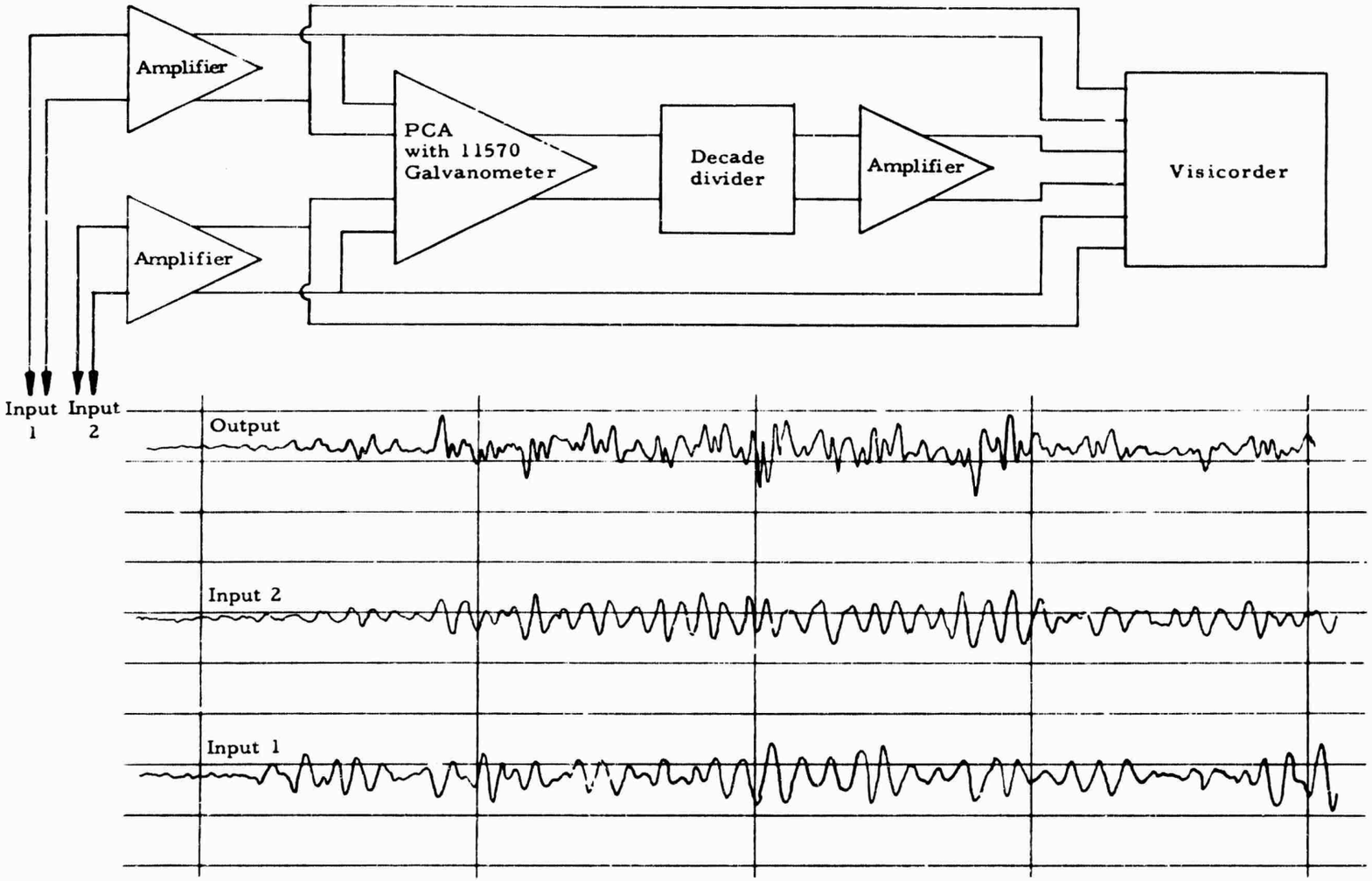

Figure 22. Tracing of Visicorder record, computing-galvanometer response to earthquake inputs, multiplication-correlation connection

Suspension	
Resonant frequency (in air)	20.0 Hz
Resonant frequency (in fluid)	8.2 Hz
Sensitivity (series connection)	$1.82 \times 10^{-7} A^2/mm/m$
Flat frequency response (0.7 critically damped)	0-4.8 Hz within 5%
Damping fluid	
Type	Silicone DC200
Viscosity (for 0.7 of critical damping)	$2.044 \times 10^{-5} m^2/sec$
Density	$955.0 kg/m^3$
Refractive index	1.400
Optics	
Mirror size	1.59 mm wide x 6.35 mm long
Lens focal length	496 mm
Galvanometer focal length	125 mm
Galvanometer pupil (vertical plane)	0.873 rad (50 deg)
Physical	
Height	100 mm
Diameter	57.2 mm
Weight	0.296 kg (0.65 lbs)

3.4 CONCLUSIONS AND RECOMMENDATIONS

The computing galvanometer operates in accordance with the initial design intent. Its usefulness in seismic analysis is left for the seismologist to determine.

It is recommended that the Computing Galvanometer, Model 11570, be installed in a Model 16956 photocell amplifier and be delivered to a seismic observatory for evaluation.

4. HIGH-RESOLUTION GALVANOMETER

4.1 GENERAL

The effective sensitivity of a galvanometer with a rotating plane or spherical mirror and with several simple combinations of lenses will be discussed in this section. It will be necessary to keep in mind the basic principles employed in the optical systems of galvanometer light-beam instruments. There are two types of these instruments in general use: the photographic recorder which generally employs a light source, converging lens, and galvanometer with a flat mirror to focus a light spot onto photosensitive paper, and the phototube or photocell amplifier which electronically amplifies changes in light intensity because of galvanometer mirror rotation. This latter system commonly uses two photosensors in a bridge or differential circuit, with a beam splitter to divide the light between them. The light source can be focused onto the beam splitter, but there are advantages to inserting an aperture stop between the source and galvanometer mirror and focusing this aperture on the splitter; then the source can be focused on the rotating mirror so that its image on the detecting cells does not move.

The requirements for practical systems are that the final image must be real (i. e., a real image on the photographic paper or on the beam splitter) and that the lateral magnification must be a practical value.

4.2 OPTICAL MAGNIFICATION

4.2.1 Linear Lateral Magnification

The linear lateral magnification of a single lens or mirror determines the object-to-image size ratio, as well as the change in position of the image for a corresponding motion of the object. For both lenses and mirrors, the linear lateral magnification is defined as

$$M = \frac{h'}{h} = -\frac{s'}{s};$$

also $$\frac{\Delta h'}{\Delta h} = M.$$

The symbols are identified in figure 23, and quantities are positive when measured as shown.

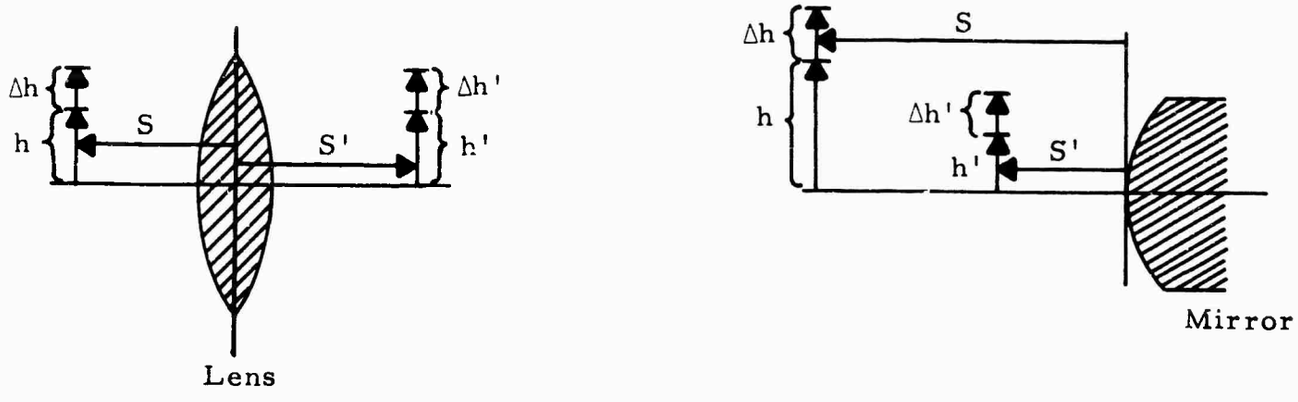

Figure 23. Symbols used for mirrors and lenses

4.2.2 Rotational Magnification

Rotational magnification is defined as the ratio of the change in image position to the corresponding change in angle of rotation of the element forming the image:

$$M_R = \frac{\Delta h'}{\Delta \alpha} .$$

These quantities are shown in figure 24 for a flat mirror.

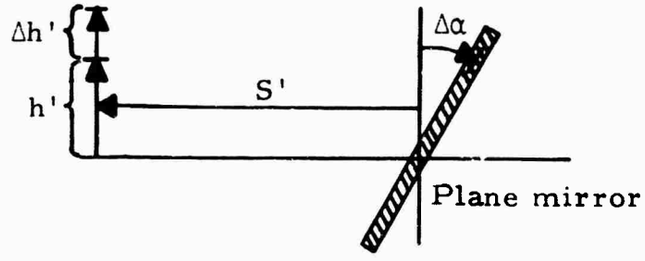

Figure 24. Rotational magnification of a plane mirror

The rotational magnification of plane and spherical mirrors is

$$M_R = \frac{\Delta h'}{\Delta \alpha} = 2S' \frac{Rr}{Rm},$$

where Rr is the radius of rotation and Rm is the radius of the mirror. These quantities are shown in figure 25 for a convex mirror. The expression for rotational magnification of spherical mirrors applies, except for sign, to both convex and concave mirrors mounted in any position, and when Rr = Rm, it applies to flat mirrors also.

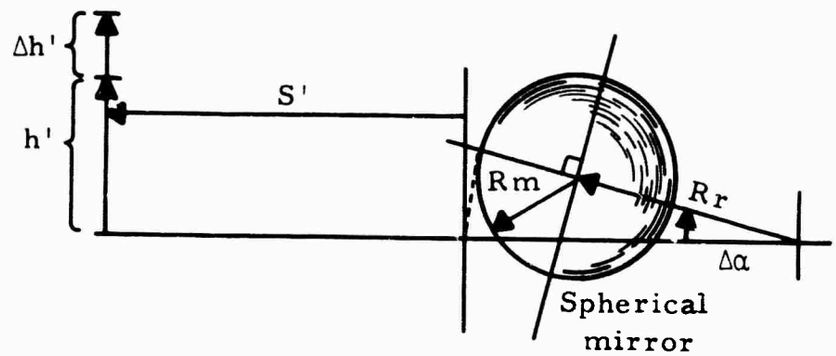

Figure 25. Rotational magnification of a spherical mirror

4.3 OPTICAL SYSTEMS

4.3.1 General

In this section, the galvanometer with a plane mirror and no optical elements between the mirror and image will be taken as a reference for the rotational magnification or sensitivity of other systems. All systems will be required to produce an accessible real image. Although the practical usefulness of any system will depend on its lateral magnification and its object-position requirements for a real image, the rotational magnification begins at the moving mirror and is independent of the manner in which light is furnished to the mirror. The position and size of the object of the galvanometer mirror is the first parameter affecting the overall system sensitivity.

4.3.2 Galvanometer with a Plane Mirror

4.3.2.1 Single Reflection

The rotational magnification of a flat mirror was given in section 4.2.2 as

$$M_R = \frac{\Delta h'}{\Delta \alpha} = 2S'.$$

It is directly proportional to image distance. A flat mirror requires a virtual object to form a real image.

4.3.2.2 Multiple Reflections

The rotational magnification of a stationary plane mirror combined with a rotating plane mirror such that the light beam is deflected from the rotating mirror n times is

$$M_R = \frac{\Delta h'}{\Delta \alpha} = 2n\,[S' + (n-1)\,d].$$

Note that there is a discontinuity at d = o. The symbols are in figure 26: S' is the final image distance from the vertex of the rotating mirror and d is the spacing between the rotating and the stationary mirror.

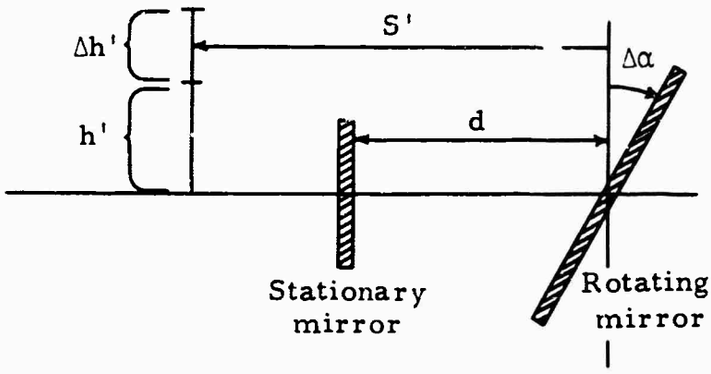

Figure 26. Multiple reflections from a plane mirror

A small mirror spacing is generally necessary if the maximum useable rotation angle of the galvanometer mirror is not to be excessively limited. For a deflection-doubling mirror inside of a galvanometer case, S' would be much larger than d, so that the sensitivity would be nearly doubled for any given distance.

4.3.3 Galvanometer with a Spherical Mirror

The rotational magnification of a spherical galvanometer mirror was given in section 4.2.2 as

$$M_R = \frac{\Delta h'}{\Delta \alpha} = 2S' \frac{Rr}{Rm}.$$

Figure 27 indicates the nonlinearities of this system in terms of mirror-rotation angle and beam-deflection angle; the actual beam deflection is

$$\sin\left(\frac{\theta}{2}\right) = \frac{Rr}{Rm} \sin \alpha,$$

where the angles and radii are identified in figure 27.

4.3.4 Galvanometer and Lens

4.3.4.1 General

It is obvious, from the laws of image formation and the need to project a real image, that a converging optical element is necessary at some point in the light path between real source and real image when the galvanometer has a plane mirror. Since the usual practice is to make this converging element a lens mounted on the galvanometer case, it falls within the province of the galvanometer designer, and since this lens can affect the overall galvanometer sensitivity, we will examine it in some detail. There are three possible arrangements, as shown in figure 28.

4.3.4.2 Single-Pass Lens and Plane Mirror

A single converging lens can be placed in the light path either before or after the galvanometer mirror. In referring to figure 28a, the rotational magnification of the first system is

$$\frac{\Delta h'}{\Delta \alpha} = 2S'$$

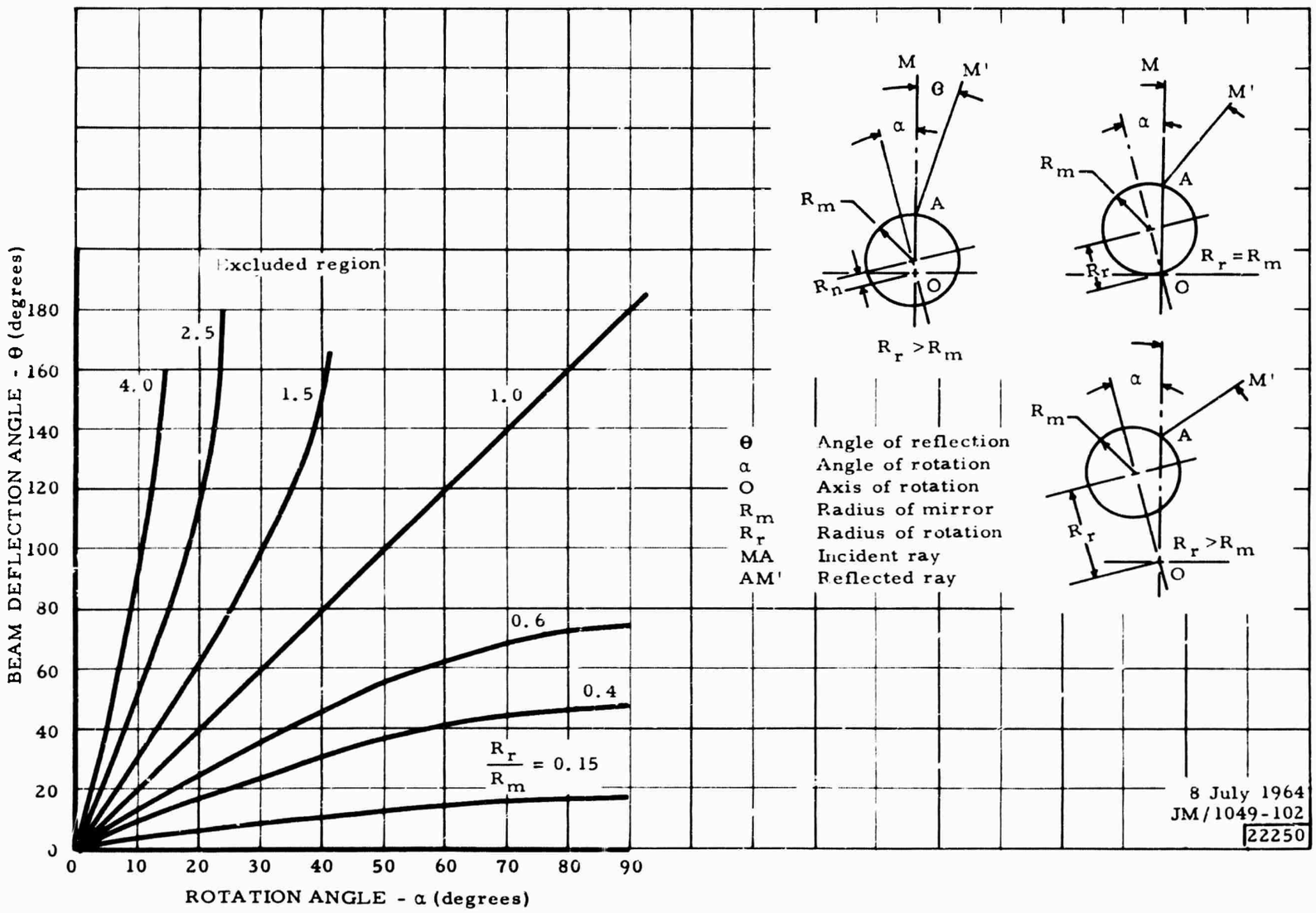

Figure 27. Rotating spherical mirror deflection characteristics

where S' will be the distance from the rotating mirror's vertex to the final image, and $\Delta h'$ will be the change in final image displacement caused by mirror rotation of $\Delta\alpha$ radians.

The rotational magnification of the second system, figure 28, is

$$\frac{\Delta h'}{\Delta \alpha} = 2\left[S'\left(1 - \frac{d}{f}\right) + \frac{d^2}{f}\right]$$

where the s bols d and f refer to the lens-to-mirror spacing and the lens focal lengt spectively. This expression can be made more useful by referring i onfiguration 28a. The ratio will indicate the relative effect a lens has on sensitivity for any given image distance. Thus, calling the ratio R, we have

$$R = \frac{2\left[S'\left(1 - \frac{d}{f}\right) + \frac{d^2}{f}\right]}{2S'}$$

$$R = 1 - \frac{d}{f}\left(1 - \frac{d}{S'}\right)$$

The term $\frac{d}{S'}$ will always be positive but less than unity for a real image, so that for a particular image distance, the ratio R depends essentially on the value of $\frac{d}{f}$. Since we must exclude a diverging lens (negative focal length), there are two distinct possibilities: f may be greater than or less than $\frac{d}{2}$.

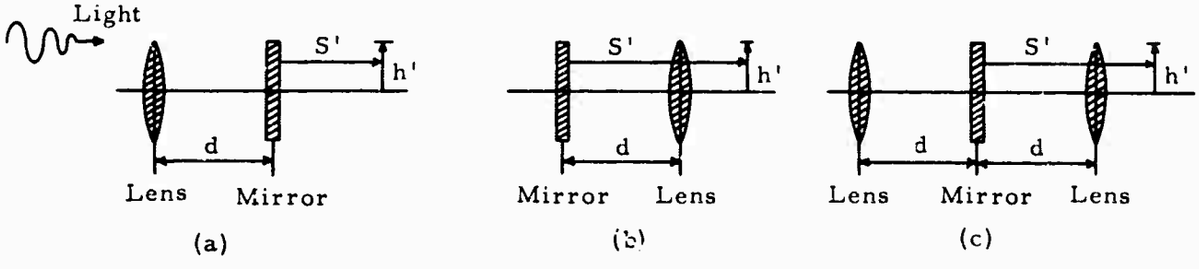

Figure 28. Plane mirror and lens combinations

When f is greater than $\frac{d}{2}$ (as it generally is in practice), there will always be a reduction in sensitivity when a lens is placed in front of a galvanometer and the image distance from the galvanometer mirror held constant. However, when f is positive but less than $\frac{d}{2}$, it is possible for the absolute value of R to be greater than unity. In this case, the sensitivity of the plane mirror and lens combination would be greater than that of the plane mirror alone for any given image distance. This arrangement allows high sensitivity to be achieved by having the object of the lens placed between the lens and the mirror (a virtual object).

The systems discussed in this section are summarized in figure 29. Figure 29a is the reference arrangement, and has a magnification higher than 29b but lower than 29c. However, the image in 29c is very sensitive to changes in object position or mirror focal length, and in addition, this system must be furnished with a virtual object. Also, the small $\frac{f}{d}$ ratio would effectively require that the lens have a small diameter if mounted close to the galvanometer, and, therefore, possibly act as an aperture stop.

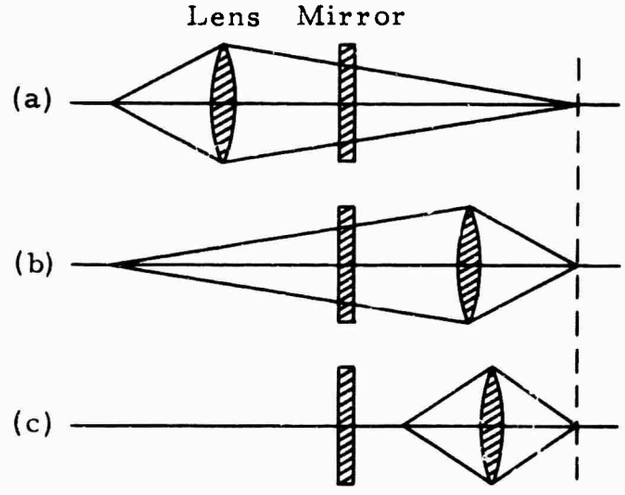

Figure 29. Comparison of single-pass lens systems

4.3.4.3 Double-Pass Lens and Plane Mirror

A galvanometer and double-pass lens system is shown in figure 30. This arrangement of the system is convenient from a construction standpoint because the lens may be mounted on the galvanometer case. A relatively large-diameter lens may be used because the system focal length is (in the usual case) less than the lens focal length.

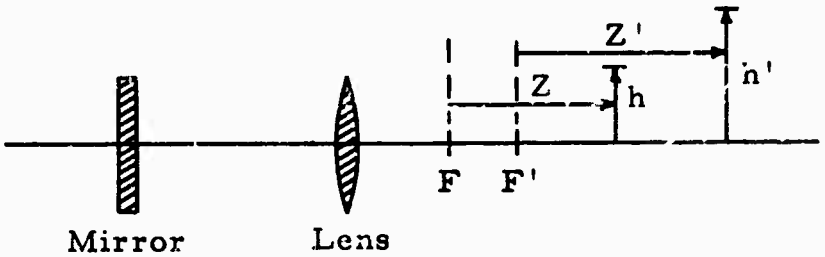

Figure 30. Double-pass lens system

In sensitivity, the double-pass system is equivalent to the single-pass system of either figure 29b or 29c, depending on the value of $\frac{f}{d}$, where f is the lens focal length and d is the lens-to-mirror spacing.

The complete object-image relationship for a double-pass lens system is best handled by finding the position of the principal focal planes of the system and by using Newton's equation $ZZ' = FF'$. Z and Z' are distances measured from the primary focal points F and F' of the system (which fall together if the light beam enters and leaves the system through the same lens) and are positive when measured to the right as in figure 30. The product ff' is equal to $\frac{f}{2(f-d)}$ (which is always positive, indicating that Z and Z' always have the same sign), and the distance from the mirror to the system focal plane is $F = F' = \frac{\left(f_L^2 - 2d^2\right)}{2(f_L - d)}$ as before, f_L is the lens focal length and d is the lens-to-mirror spacing.

4.3.4.4 Spherical Mirror and Lens

Because the expressions for rotational magnification or sensitivity of spherical and of plane mirrors as introduced in section 4.2.2 are similar, we can say that the sensitivity of a spherical mirror followed by a lens is equal to the

sensitivity of a plane mirror in the same system, multipled by the factor $\frac{Rr}{Rm}$ which applies to the spherical mirror. The same considerations as to lens focal length and placement, discussed in section 4.3.4 apply. The type of mirror to be used depends on the desired object-image relation of the mirror and lens combination, and also on mechanical factors.

4.3.5 Stationary Curved Mirrors

There is a possibility of reflecting the light beam from the galvanometer mirror to a stationary curved mirror to increase the overall beam deflection. The sensitivity-multiplying factor for such a mirror would be its lateral magnification. Within the limits of linearity and image distortion, spherical mirrors can be used for this purpose.

4.4 SOME PRACTICAL CONSIDERATIONS

In general, the lateral magnification of an optical system is chosen to be close to unity. When a simple lens follows the galvanometer mirror and is closely spaced to the mirror (such that $\frac{f}{d}$ is large), the system sensitivity is typically reduced approximately 15 to 20% from what would be obtainable with the galvanometer mirror alone. However, double-pass lens systems have the important advantage of comparatively short focal lengths. When the lateral magnification is one, the object and image are closer to the galvanometer.

A major problem in galvanometers, particularly those with stiff suspensions, is distortion of the mirror upon rotation. A plane mirror is least affected (its focal length is changed the least) by a given amount of bending. In high-frequency galvanometers, the coil is generally wound around or otherwise attached directly to the mirror so that if a curved mirror were placed in one of these units (especially if the spring constant had to be increased to compensate for increased inertia) there could be a serious problem.

4.5 CONCLUSIONS

The placement and form of optical elements following the galvanometer mirror have a significant effect on system sensitivity. Alternate arrangements to the usual procedure of mounting a lens directly in front of the rotating mirror should be considered. A reflection-doubling mirror mounted close to the rotating mirror is the most promising method of increasing galvanometer sensitivity. A spherical rotating mirror will be practical for values of $\frac{Rr}{Rm}$ close to unity.